arXiv:1108.6312v1 [cs.IT] 31 Aug 2011

Computation Alignment: Capacity Approximation without Noise Accumulation

Urs Niesen, Bobak Nazer, and Phil Whiting

Abstract

Consider several source nodes communicating across a wireless network to a destination node with the help of several layers of relay nodes. Recent work by Avestimehr *et al.* has approximated the capacity of this network up to an additive gap. The communication scheme achieving this capacity approximation is based on compress-and-forward, resulting in noise accumulation as the messages traverse the network. As a consequence, the approximation gap increases linearly with the network depth.

This paper derives a capacity approximation for multi-layer wireless relay networks with an approximation gap that is independent of the network depth and dependent only on the number of source nodes and the fading statistics. This is achieved by a new communication strategy termed *computation alignment*. This strategy is based on the compute-and-forward framework, which enables relays to decode deterministic functions of the transmitted messages. Alone, compute-and-forward is insufficient to approach the capacity as it incurs a penalty for approximating the wireless channel with complex-valued coefficients by a channel with integer coefficients. Here, this penalty is avoided by breaking the wireless channel into several subchannels combined with a signal-alignment strategy to ensure that these subchannels have integer channel coefficients.

I. INTRODUCTION

Consider a line network, consisting of a single source communicating to a single destination via a sequence of relays connected by point-to-point channels. The capacity of this simple relay network is achieved by decode-and-forward and is determined solely by the weakest of the point-to-point channels. As a consequence, the performance of the optimal scheme is unaffected by noise accumulation, regardless of the length of the relay network. This raises the question whether the same holds true in general multi-user wireless relay networks, i.e., if the capacity depends on the network depth. In this paper, we investigate this question in the context of multiple sources communicating with a single destination across a multi-layer wireless relay network.

A. Motivation and Summary of Results

In a multi-layer wireless relay network, each relay observes a noisy linear combination of the signals transmitted by the relays in the previous layer. In order to avoid noise accumulation, the relays should perform some type of decoding to eliminate noise at each layer. One natural approach, decode-and-forward, is for each layer of relays to decode the messages sent by the previous layer and retransmit them, just as in the line network mentioned above. Unfortunately, while the performance of this scheme is independent of the network depth, it is often interference limited and, as a result, its performance can diverge significantly from the capacity.

Instead of combating interference, as is done in the decode-and-forward approach, other communication strategies embrace the signal interactions introduced by the wireless channel. One such strategy is compress-and-forward, in which each relay transmits a compressed version of its received signal. Such strategies can offer significant advantages over decode-and-forward. Indeed, recent work by Avestimehr *et al.* [1] has shown that, for the class of multi-layer wireless relay networks with single destination

---

U. Niesen and P. Whiting are with the Mathematics of Networks and Communications Research Department, Bell Labs, Alcatel-Lucent. B. Nazer is with the ECE Department, Boston University. Emails: urs.niesen@alcatel-lucent.com, bobak@bu.edu, pwhiting@research.bell-labs.com.

This work was supported in part by AFOSR under grant FA9550-09-1-0317.

considered here, compress-and-forward approximately achieves capacity up to a gap independent of the power constraints at the nodes in the network. However, since the compress-and-forward scheme does not remove noise at each relay, noise accumulates from one layer in the network to the next. As a consequence, the approximation gap in [1] (and related ones such as those based on noisy network coding [2]) increases linearly with the number of layers in the relay network. Thus, as the depth of the network increases, the approximation guarantee becomes weaker.

In this paper, we make progress on this issue by deriving a new capacity approximation result for the multi-layer relay network with an approximation gap dependent only on the number of source nodes in the network and on the fading statistics, but independent of the depth of the network. In other words, unlike the approximation result in [1], the approximation guarantee here is not affected by increasing the depth of the relay network.

Our approach is built around the compute-and-forward framework proposed by [3]. In this framework, each transmitter encodes its message into a codeword drawn from the same lattice codebook. As a result, all integer combinations of codewords are themselves codewords, enabling relays to decode linear functions of the transmitted codewords rather than treating interference as noise. While the use of lattice codes seems like a natural fit for this setting, it alone is insufficient to approach the network capacity, as was shown recently in [4]. The primary reason is that this scheme approximates the wireless channel with complex-valued channel gains by a channel with integer-valued channel gains. The residual signals not captured by this integer approximation are treated as additional noise. It is this additional noise that ultimately limits the performance of this scheme in the high signal-to-noise ratio (SNR) regime. This obstacle was overcome in [4] in the high SNR limit by combining compute-and-forward with the rational alignment scheme due to Motahari *et al.* [5]. For the time-varying channels considered here, we propose a new scheme, termed *computation alignment*, that allows for a much sharper analysis at finite SNRs. Our scheme couples compute-and-forward with a signal-alignment scheme inspired by ergodic interference alignment [6]. This approach decomposes the wireless channel with time-varying complex-valued channel gains into several subchannels with constant integer-valued channel gains, over which lattice codes can be employed efficiently.

B. Related Work

Relay networks have been the subject of considerable interest. For *wired* networks (i.e., networks of point-to-point channels), Koetter *et al.* recently proved that it is capacity-optimal to separate channel and network coding [7]. It is now well known that routing over the resulting graph of bit pipes is optimal for unicasting [8], [9] and, as demonstrated by Ahlswede *et al.* [10], network coding is required to achieve the multicast capacity.

For *wireless* networks, channel-network separation is not always optimal: higher rates can be achieved using more sophisticated relaying techniques such as compress-and-forward (see, e.g., [1], [2], [11]–[13]), amplify-and-forward (see, e.g., [14]–[18]), and compute-and-forward (see, e.g., [3], [4], [19], [20]). While for certain classes of deterministic networks the unicast and multicast capacity regions are known [1], [21], [22], in the general, noisy case, these problems remain open. Recent progress has been made by focusing on finding capacity approximations [1], [23]–[26].

As mentioned above, our approach combines signal alignment with lattice coding techniques. Signal alignment for interference management has proved useful especially for the Gaussian interference channel [5], [6], [24], [27]–[29]. Recent work has developed alignment schemes that attain the maximum degrees of freedom of certain Gaussian multi-hop networks [30]–[33].

Lattice codes provide an elegant framework for many classical Gaussian multi-terminal problems [34], [35]. Beyond this role, it has recently been shown that they have a central part to play in approaching the capacity of networks that include some form of interference [3], [19], [20], [24], [29], [36], [37].

C. Organization

The remainder of this paper is organized as follows. Section II introduces the problem setting as well as notation. Section III presents the main results. Sections IV–VIII contain proofs. Section IX concludes the paper.

II. PROBLEM SETTING AND NOTATION

This section formally introduces the problem setting and notation. Although we are interested here in relay networks with several layers, it will be convenient to first discuss networks with a single layer. This single-layer network model is presented in Section II-B. We then apply the insights obtained for networks with a single layer of relays to networks with more than one layer of relays. This multi-layer network model is presented in Section II-C. Before we formally describe these two problem settings, we introduce some notational conventions in Section II-A.

A. Notational Conventions

Throughout this paper, $\log$ denotes the logarithm to the base two, and all capacities and rates are hence expressed in terms of bits. We use bold font lower and upper case, such as $\boldsymbol{h}$ and $\boldsymbol{H}$, to denote vectors and matrices, respectively. Realizations of random variables will be denoted by sans-serif font, e.g., H is a realization of the random matrix variable $\boldsymbol{H}$.

B. Single-Layer Relay Networks

We start with a model for a wireless relay network with a single layer. This single layer is to be interpreted as a part of a larger relay network, to be introduced formally in Section II-C. The single-layer relay network consists of K transmitters and K receivers as depicted in Fig. 1. We think of the K transmitters as being located at either the source nodes or at the relay nodes in some layer, say d, of the larger relay network. We think of the K receivers as being located at either the destination nodes or at the relay nodes at layer $d+1$ of the larger relay network.

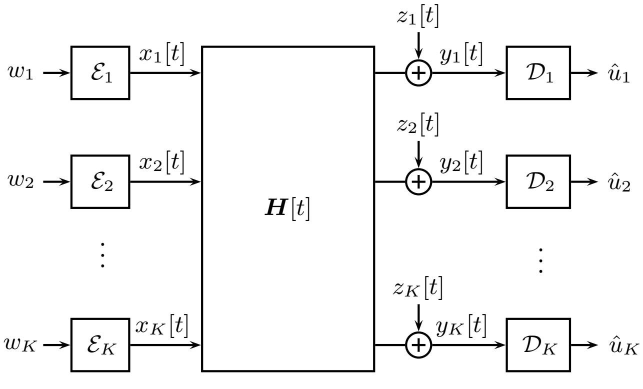

Fig. 1. K transmitters communicate an invertible set of functions $u_k = f_k(w_1, w_2, \dots, w_K)$ of their messages to K receivers over a time-varying interference channel.

Each transmitter, indexed by $k \in \{1, \dots, K\}$, has access to a *message* w_k that is generated independently and uniformly over $\{1, \dots, 2^{TR_k}\}$, where R_k is the *rate* of transmitter k. Each receiver, indexed by $m \in \{1, \dots, K\}$, aims to recover a *deterministic function*

$$u_m \triangleq f_m(w_1, \dots, w_K)$$

of the K messages $(w_1, \dots, w_K)$. We impose that the functions $(f_m)_{m=1}^K$ computed at the receivers are *invertible*. In other words, there must exist a function g such that $g(u_1, u_2, \dots, u_K) = (w_1, w_2, \dots, w_K)$.

Since the functions to be computed at the receivers are deterministic, noise is prevented from accumulating as messages traverse the larger relay network. Moreover, since the functions to be computed are invertible, no information is lost from one layer to the next in the larger relay network.

The transmitters communicate with the receivers over a Rayleigh-fading complex Gaussian channel modeled as follows. The *channel output* $y_m[t] \in \mathbb{C}$ at receiver $m \in \{1, \dots, K\}$ and time $t \in \mathbb{N}$ is given by

$$y_m[t] \triangleq \sum_{k=1}^{K} h_{m,k}[t] x_k[t] + z_m[t], \tag{1}$$

where $x_k[t] \in \mathbb{C}$ is the *channel input* at transmitter k, $h_{m,k}[t]$ is the *channel gain* between transmitter k and receiver m, and $z_m[t]$ is *additive receiver noise*, all at time t. The noise $z_m[t]$ is circularly-symmetric complex Gaussian with mean zero and variance one, and independent of the channel inputs $x_k[t]$ for $k \in \{1, \dots, K\}$, $t \in \mathbb{N}$, and independent of all other $z_{m'}[t']$ for $(m', t') \neq (m, t)$. Each channel gain $h_{m,k}[t]$ is assumed to be circularly-symmetric complex Gaussian, with mean zero and variance one, i.e., we assume Rayleigh fading. As a function of t, $(h_{m,k}[t])_{t \in \mathbb{N}}$ is a stationary ergodic process for every m and k. The K^2 processes $(h_{m,k}[t])_{t \in \mathbb{N}}$ are mutually independent as a function of m, k. Denoting by

$$\boldsymbol{H}[t] \triangleq (h_{m,k}[t])_{m,k}$$

the matrix of channel gains at time t, this implies that the matrix process

$$\boldsymbol{H}[1], \boldsymbol{H}[2], \boldsymbol{H}[3], \dots$$

is also stationary and ergodic. The channel gains $\boldsymbol{H}[t]$ are known at all nodes in the network at time t. In other words, we assume availability of full causal channel state information (CSI) throughout the network.

Each transmitter consists of an *encoder* $\mathcal{E}_k$ mapping its message w_k into a sequence of T channel inputs

$$(x_k[t])_{t=1}^{T} \triangleq \mathcal{E}_k(w_k),$$

satisfying an *average power constraint*

$$\frac{1}{T} \sum_{t=1}^{T} |x_k[t]|^2 \leq P.$$

Each receiver consists of a *decoder* $\mathcal{D}_m$ mapping its observed channel output into an estimate

$$\hat{u}_m \triangleq \mathcal{D}_m(y_m[1], \dots, y_m[T])$$

of the desired function $u_m = f_m(w_1, \dots, w_K)$. Let

$$p_e \triangleq \mathbb{P}\big(\textstyle\bigcup_{m=1}^{K} \{\hat{u}_m \neq u_m\}\big)$$

denote the average probability of error across all relays.

Definition. A computation sum rate $R(P)$ is *achievable* if, for every $\varepsilon > 0$ and every $T \geq T_0(\varepsilon)$, there exist encoders with blocklength T, average power constraint P, and rates satisfying $\sum_{k=1}^{K} R_k \geq R(P)$, and there exist decoders computing some invertible deterministic function $(f_m)_{m=1}^{K}$ with probability of error $p_e \leq \varepsilon$. The *computation sum capacity* $C(P)$ of the single-layer relay network is the supremum of all achievable computation sum rates $R(P)$.

Observe that the definition of computation sum capacity does not prescribe the function of the messages to be computed at the receivers. The only requirement is that these functions are deterministic and invertible. In other words, the computation sum capacity is the largest sum rate at which *some* (as opposed to *any*) such function can be computed reliably.

C. Multi-Layer Relay Networks

Having described the single-layer network setting, we now turn attention to networks with multiple layers of relays. These networks consists of a concatenation of D single-layer networks as defined in Section II-B. The network contains K source nodes at layer zero connected through a Rayleigh-fading channel to K relay nodes at layer one. Layer d in the network contains K relay nodes connected through a Rayleigh-fading channel to K relay nodes at layer $d+1$. The relay nodes at layer D are connected to the destination node at layer $D+1$ through orthogonal bit pipes of infinite capacity. This ensures that the intermediate relay layers, not the bit pipes, are the bottleneck in the network. This scenario is depicted in Fig. 2.

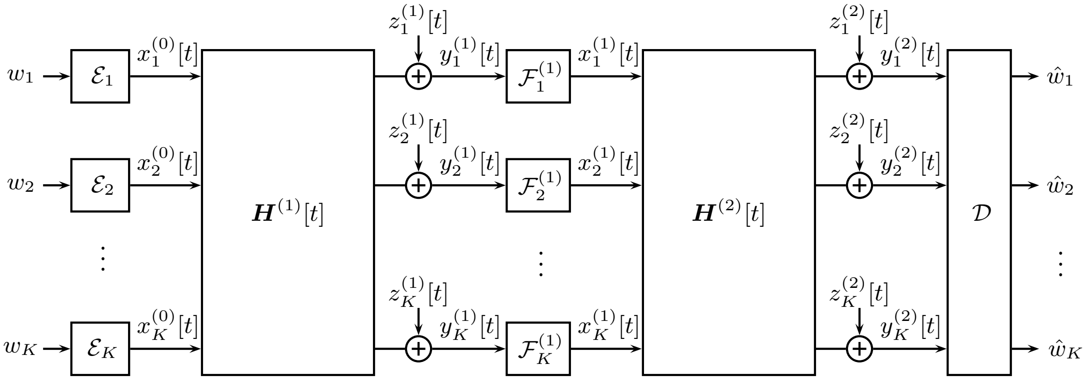

Fig. 2. A multi-layer relay network with $D = 2$ layers and K relays per layer.

Formally, each transmitter at a source node, indexed by $k \in \{1, \dots, K\}$, has access to a *message* w_k of rate R_k that is generated independently and uniformly over $\{1, \dots, 2^{TR_k}\}$. The receiver at the destination node aims to recover the transmitted messages $(w_1, w_2, \dots, w_K)$.

The transmitters at layer $d \in \{0, \dots, D-1\}$ communicate with the receivers at layer $d+1$ over a Rayleigh-fading complex Gaussian channel modeled as in the single-layer case. The *channel output* $y_m^{(d+1)}[t] \in \mathbb{C}$ at the receiver at relay $m \in \{1, \dots, K\}$ in layer $d+1$ and time $t \in \mathbb{N}$ is given by

$$y_m^{(d+1)}[t] \triangleq \sum_{k=1}^{K} h_{m,k}^{(d+1)}[t] x_k^{(d)}[t] + z_m^{(d+1)}[t],$$

where $x_k^{(d)}[t]$ is the *channel input* at the transmitter at relay or source $k \in \{1, \dots, K\}$ at layer d. The *channel gains* $h_{m,k}^{(d+1)}[t]$ and the *additive noise* $z_m^{(d+1)}$ satisfy the same statistical assumptions as in the single-layer network, see (1), and are assumed to be independent across different layers. As mentioned earlier, the receiver at the relay nodes in layer D are connected to the destination node at layer $D+1$ through K orthogonal bit pipes with infinite capacity. Without loss of generality, we can assume that the relays in layer D simply forward their observed channel outputs $y_m^{(D)}[t]$ to the destination node.

Each transmitter at source node k consists of an *encoder* $\mathcal{E}_k$ mapping its message w_k into a sequence of T channel inputs,

$$(x_k^{(0)}[t])_{t=1}^{T} \triangleq \mathcal{E}_k(w_k),$$

satisfying an *average power constraint*

$$\frac{1}{T} \sum_{t=1}^{T} |x_k^{(0)}[t]|^2 \leq P.$$

The receiver-transmitter pair at relay node k in layer $d \in \{1, \dots, D-1\}$ consists of a *relaying function* $\mathcal{F}_k^{(d)}$ mapping the block of observed channel outputs $(y_m^{(d)}[1], \dots, y_m^{(d)}[T])$ from layer d into a block of channel inputs

$$(x_k^{(d)}[t])_{t=1}^T \triangleq \mathcal{F}_k^{(d)}(y_m^{(d)}[1], \dots, y_m^{(d)}[T])$$

for layer $d+1$, satisfying an average power constraint

$$\frac{1}{T}\sum_{t=1}^{T} |x_k^{(d)}[t]|^2 \leq P.$$

As may be seen from the definition of the relaying function, we do not impose causality for the operations at the relay. This assumption is only for ease of notation—since we are dealing with a layered network, all results are also valid for causal relaying functions by coding over several blocks.

Finally, the receiver at the destination node in layer $D+1$ consists of a *decoder* $\mathcal{D}$ mapping its observed channel outputs (forwarded from the relays at layer D) into an estimate

$$(\hat{w}_1, \hat{w}_2, \dots, \hat{w}_K) \triangleq \mathcal{D}\big((y_1^{(D)}[1], \dots, y_1^{(D)}[T]), \dots, (y_K^{(D)}[1], \dots, y_K^{(D)}[T])\big)$$

of the messages $(w_1, \dots, w_K)$. Let

$$p_e \triangleq \mathbb{P}\big(\textstyle\bigcup_{k=1}^K \{\hat{w}_k \neq w_k\}\big)$$

denote the average probability of decoding error.

Definition. A sum rate $R^{(D)}(P)$ is *achievable* if, for every $\varepsilon > 0$ and every $T \geq T_0(\varepsilon)$, there exist encoders, relaying functions, and a decoder with blocklength T, average power constraint P, rates satisfying $\sum_{k=1}^K R_k \geq R^{(D)}(P)$, and probability of error $p_e \leq \varepsilon$. The *sum capacity* $C^{(D)}(P)$ of the multi-layer relay network is the supremum of all achievable sum rates $R^{(D)}(P)$.

It is worth pointing out that $C^{(D)}(P)$ with $D = 1$ as defined here and $C(P)$ defined in Section II-B are, in general, not equal. In fact, $C^{(1)}(P)$ is the rate achievable over a single-layer network with a *centralized* decoder (having access to all the channel outputs at the K relays) at the destination node aiming to recover all K transmitted messages. On the other hand, $C(P)$ is the rate achievable over a single-layer network with K *decentralized* decoders at the relays aiming to recover an invertible function of the K transmitted messages. Clearly, any such decentralized set of decoders can be used to implement a centralized decoder by concatenating them with an inverter. Hence $C^{(1)}(P) \geq C(P)$. However, we do not have equality in general.

III. MAIN RESULTS

As the main results of this paper, we provide an approximate characterization of the computation sum capacity $C(P)$ of the single-layer relay network (Section III-A), and an approximate characterization of the sum capacity $C^{(D)}(P)$ of the D-layer relay network (Section III-B).

A. Single-Layer Relay Networks

We start with the analysis of the computation sum capacity $C(P)$ of a single-layer relay network consisting of K source nodes and K relay nodes.

Theorem 1. *For a time-varying single-layer network with $K \geq 2$ source nodes and K relay nodes, the computation sum capacity $C(P)$ is lower and upper bounded as*

$$K\log(P) - 7K^3 \leq C(P) \leq K\log(P) + 5K\log(K)$$

for every power constraint $P \geq 1$.

The proof of the lower bound in Theorem 1 is presented in Sections V (for $K = 2$) and VI (for $K > 2$). The proof of the upper bound in Theorem 1 is presented in Section VII.

Theorem 1 provides an approximate characterization of the computation sum capacity $C(P)$ of the single-layer relay network. Comparing the upper and lower bounds shows that the approximation is up to an additive gap of $7K^3 + 5K\log(K)$ bits/s/Hz. In particular, the gap does not depend on the power constraint P. In other words, Theorem 1 asserts that

$$C(P) = K\log(P) \pm O(1).$$

This is considerably stronger than the best previously known bounds in [4] on the computation sum capacity of such networks, which only provide the degrees-of-freedom approximation

$$C(P) = K\log(P) \pm o(\log(P))$$

as $P \to \infty$.

The upper bound in Theorem 1 results from the cut-set bound, allowing cooperation among the sources and among the relays. This transforms the channel into a $K \times K$ multiple-input multiple-output system, and the upper bound follows from analyzing its capacity. From Theorem 1, we hence see that computation of a (carefully chosen) invertible function can be performed in a distributed manner with at most a $O(1)$ loss in rate compared to the centralized scheme in which the K transmitters cooperate and the K receivers cooperate.

The communication scheme achieving the lower bound in Theorem 1 is based on a combination of a lattice computation code with a signal-alignment strategy, which we term *computation alignment*. We now provide a brief description of these two components and how they interact—the details of the argument can be found in the proof of Theorem 1 in Sections V and VI.

A *lattice* is a discrete subgroup of $\mathbb{R}^T$, and hence has the property that any integer linear combination of lattice points is again a lattice point. A *lattice computation code* as defined in [3] uses such a lattice, intersected with an appropriate bounding region to satisfy the power constraint, as its codebook. Assume for the moment that the channel gains $\boldsymbol{H}$ are all integers. Then the receivers observe an integer linear combination of codewords plus Gaussian noise. By the lattice property, this is equal to some other codeword plus noise. If the lattice is carefully chosen, the receivers can remove the noise, and are hence left with the integer combination of the codewords—thus decoding a deterministic function of the messages.

While this approach is close to optimal for channels with integer channel gains $\boldsymbol{H}$, it was shown in [4] that this approach performs quite poorly for general real or complex channel gains in the high SNR regime. The reason for the poor asymptotic performance of the lattice scheme is that only *integer* linear combinations of lattice codewords result in a codeword. For general real or complex channel gains, the linear combinations of the codewords computed by the channel do not result in another codeword. The residual interference resulting from this effect ultimately limits the performance of lattice computation codes as the signal-to-noise ratio increases.

To circumvent this problem, we combine the lattice computation codes with a *signal-alignment* strategy. This signal-alignment strategy converts the channel with general complex channel gains into one with integer channel gains. Over this aligned integer channel, lattice computation codes can then be effectively used. Our *signal*-alignment strategy builds on the construction for *interference* alignment in [6] and [28].

The computation-alignment scheme is best illustrated in the $K = 2$ user case. Consider two time slots t_1 and t_2. It is easy to see that the two transmitters can reliably communicate two data streams over these two time slots, for example using time sharing. This time-sharing approach can be expressed formally by choosing transmit vectors $\boldsymbol{v}_{k,1} \in \mathbb{C}^2$ at transmitter $k \in \{1, 2\}$ with $\boldsymbol{v}_{1,1} = (1, 0)$ and $\boldsymbol{v}_{2,1} = (0, 1)$. The corresponding data stream is multiplied by this transmit vector and sent over the channel at times t_1 and t_2.

We now argue that, over two time slots, we can in fact reliably compute invertible functions of three data streams. To this end, we need to carefully match pairs of channel gains. Fix a time slot t_1, and assume we can find a second time slot t_2 such that

$$\begin{aligned} h_{1,1}[t_2] &= h_{1,1}[t_1], \\ h_{1,2}[t_2] &= h_{1,2}[t_1], \\ h_{2,2}[t_2] &= h_{2,2}[t_1], \\ h_{2,1}[t_2] &= -h_{2,1}[t_1]. \end{aligned}$$

If we choose transmit vectors

$$\begin{aligned} \boldsymbol{v}_{1,1} &= (1,\ 1), \\ \boldsymbol{v}_{1,2} &= \frac{h_{1,1}[t_1]h_{2,2}[t_1]}{h_{1,2}[t_1]h_{2,1}[t_1]}(1,\ -1) \end{aligned}$$

at transmitter two, and transmit vector

$$\boldsymbol{v}_{2,1} = \frac{h_{1,1}[t_1]}{h_{1,2}[t_1]}(1,\ 1)$$

at transmitter one, then the resulting received vectors are either equal (and hence aligned) or orthogonal, as depicted in Fig. 3. Using matched filters at the receiver, we can hence separate the channel output into two data streams. By construction, each of these data streams corresponds effectively to an additive Gaussian channel with integer channel coefficients, over which lattice computation codes can be used.

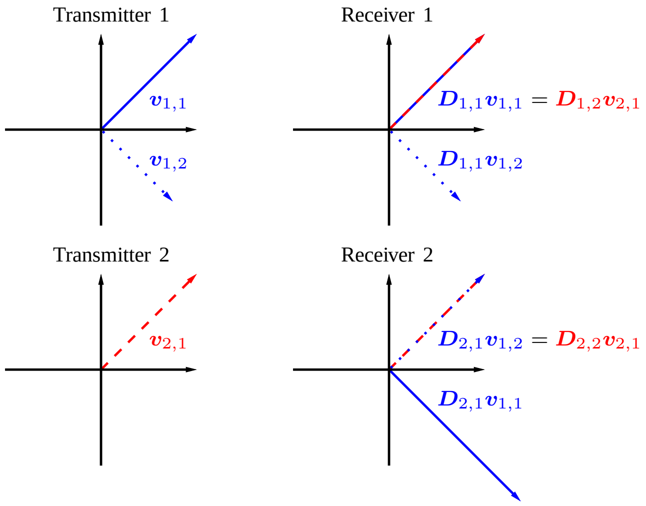
Transmitter 1
$\boldsymbol{v}_{1,1}$
$\boldsymbol{v}_{1,2}$
Receiver 1
$\boldsymbol{D}_{1,1}\boldsymbol{v}_{1,1} = \boldsymbol{D}_{1,2}\boldsymbol{v}_{2,1}$
$\boldsymbol{D}_{1,1}\boldsymbol{v}_{1,2}$
Transmitter 2
$\boldsymbol{v}_{2,1}$
Receiver 2
$\boldsymbol{D}_{2,1}\boldsymbol{v}_{1,2} = \boldsymbol{D}_{2,2}\boldsymbol{v}_{2,1}$
$\boldsymbol{D}_{2,1}\boldsymbol{v}_{1,1}$

Fig. 3. Signal alignment at the receivers. Transmitter one has two transmit vectors $\boldsymbol{v}_{1,1}, \boldsymbol{v}_{1,2}$, and transmitter two has one transmit vector $\boldsymbol{v}_{2,1}$. At receiver one, $\boldsymbol{v}_{1,1}$ and $\boldsymbol{v}_{2,1}$ are aligned. At receiver two, $\boldsymbol{v}_{1,2}$ and $\boldsymbol{v}_{2,1}$ are aligned. The figure uses the notation $\boldsymbol{D}_{m,k} = \operatorname{diag}(h_{m,k}[t_1],\ h_{m,k}[t_2])$ to express the action of the channel on the channel input over the two time slots t_1 and t_2.

Of course, matching time slots t_1 and t_2 such that the above conditions are satisfied exactly is not possible with probability one. We will instead use a quantization argument to show that this matching is possible to an arbitrary degree of accuracy. This shows that, over two time slots, we can reliably compute invertible functions of three data streams, achieving a computation sum rate of approximately $\frac{3}{2}\log(P)$. To achieve a computation rate of approximately $2\log(P)$, we consider L time slots, and show that we can reliably compute invertible functions of $2L-1$ data streams over it. This results in a computation sum rate of approximately $\frac{2L-1}{L}\log(P)$, which converges to the desired $2\log(P)$ as $L \to \infty$. The gist of the proof is similar for $K > 2$, but the arguments are more involved.

B. Multi-Layer Relay Networks

Having analyzed the computation sum capacity for single-layer relay networks, we now turn to the sum capacity of relay networks with multiple layers. Unlike the single-layer network, there is only one destination node, which is interested in recovering the original messages (and not merely a function of them). We are hence interested here in sum capacity in the traditional sense.

Theorem 2. *For a time-varying relay network with $D \geq 1$ layers, $K \geq 2$ source nodes, and K relay nodes in each layer, the sum capacity $C^{(D)}(P)$ is lower and upper bounded as*

$$K\log(P) - 7K^3 \leq C^{(D)}(P) \leq K\log(P) + 5K\log(K)$$

for every power constraint $P \geq 1$.

The proof of Theorem 2 is presented in Section VIII. The upper bound follows directly from the same cut-set bound argument as in Theorem 1. The lower bound uses compute-and-forward in each layer as analyzed in Theorem 1. The destination node gathers all the computed functions and inverts them to recover the original messages sent by the source nodes.

Theorem 2 provides an approximate characterization of the sum capacity of the D-layer relay network. The gap between the lower and upper bounds is $7K^3 + 5K\log(K)$ bits/s/Hz as in Theorem 1. This gap is again independent of the power constraint P, showing that

$$C^{(D)}(P) = K\log(P) \pm O(1).$$

Moreover, the gap in Theorem 2 is also independent of the network depth D. In other words, the approximation guarantee is uniform in the network parameter D.

It is interesting to compare this approximation result to other known capacity approximations for general Gaussian relay networks of the form considered here. For general relay networks, these bounds rely on a compress-and-forward scheme, and achieve an additive approximation gap of $4(D+1)K$ bits/s/Hz [1], [38]. Unlike the gap in Theorem 2, this gap is not uniform in the network depth D. This is due to the use of compress-and-forward: In each relay layer, the channel output, consisting of useful signal as well as additive noise, is quantized and forwarded to the next layer. Thus, with each layer additional noise accumulates, degrading performance as the network depth increases. The result is an approximation guarantee that becomes worse with increasing network depth.

Theorem 2 in this paper avoids this difficulty by completely removing channel noise at each layer in the network. This is achieved by decoding a deterministic (and hence noiseless) function of the messages at each relay. Thus, noise is prevented from accumulating as the messages traverse the network. It is this feature of compute-and-forward that enables the uniform approximation guarantee in Theorem 2.

We remark that the $7K^3$ term in the lower bound of Theorem 2 is due to the construction ensuring that all received signals are integer multiples of each other. If instead of Rayleigh fading we consider channel gains with equal magnitude and independent uniform phase fading, the lower bound in Theorem 2 can be sharpened to $K\log(P)$. Deriving capacity approximations with better dependence on K for general fading processes is an interesting direction for future work.

It is also worth mentioning that, unlike the gap presented here, the approximation gap in [1] is uniform in the fading statistics. Developing communication schemes that guarantee an approximation gap that is uniform in both the network depth and the fading statistics is therefore of interest.

Finally, like other signal alignment schemes for time-varying channels such as [28] and [6], the communication scheme proposed in this paper suffers from long delays. In particular, the delay required to establish signal alignment scales at least as 2^{K^2} in the number of users K. This limits the practicality of these schemes even for moderate values of K. Finding ways to achieve signal alignment (be it for interference management or function computation) with less delay is hence of importance.

IV. CHANNEL QUANTIZATION

The achievable scheme in Theorem 1 groups together time slots so that an appropriate linear combination of the channel outputs within each group yields a more desirable effective channel. This grouping of time slots is performed such that the corresponding channel realizations “match” in a sense to be made precise later. Since each possible channel realization has measure zero, we cannot hope for channel matrices to match exactly. Instead, we will look for channel matrices that approximately match. This approximate matching is described by considering a quantized version of the channel gains. In this section, we describe such a quantization scheme, similar to the one used for ergodic interference alignment in [6].

First, we divide the complex plane from the origin up to distance ν into concentric rings centered at the origin and with spacing $1/\nu$ for some natural number $\nu \geq 2$ to be chosen later. Then, we divide each of these ν^2 rings into $\nu^2 L$ segments with identical central angles of size $2\pi/(\nu^2 L)$ for some $L \in \mathbb{N}$ also to be chosen later. These segments serve as quantization cells for the channel coefficients. Each segment is represented by the mid-point on the bisector of the corresponding central angle (see Fig. 4). We add one additional quantization point at infinity to which all channel gains with magnitude larger than ν are mapped to. We will use frequently in the following that multiplying a quantization point by any Lth root of unity results again in a quantization point.

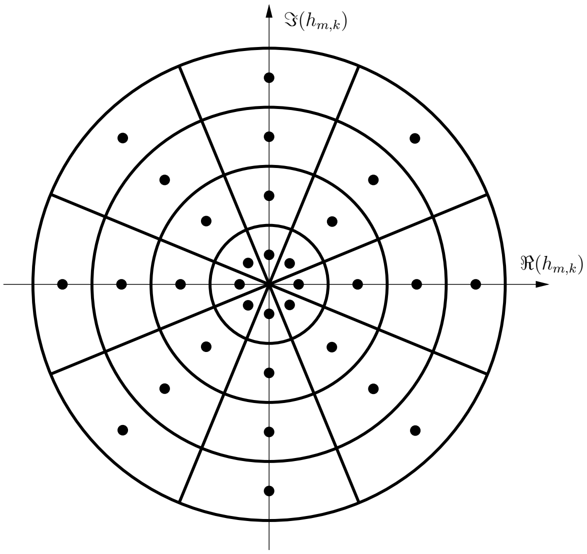

Fig. 4. Quantization scheme for channel coefficients. Coefficients up to magnitude ν are quantized by magnitude and angle. The number of angular regions is a multiple of L to ensure that multiplying a quantization point by any Lth root of unity results again in a quantization point. In the figure, $\nu = 2$ and $L = 2$

Let $\hat{h}_{m,k}[t]$ denote the quantized version of the channel coefficient $h_{m,k}[t] \in \mathbb{C}$. We then have that $\hat{h}_{m,k}[t] = \infty$ if $|h_{m,k}[t]| > \nu$, and that $\hat{h}_{m,k}[t]$ is the point in the “middle” of the quantization cell containing $h_{m,k}[t]$ otherwise (with ties broken arbitrarily). We denote by $\hat{\mathcal{H}}$ the collection of all possible quantized channel values. It will be convenient in the following to denote by

$$p_{\hat{\boldsymbol{H}}}(\hat{\mathbf{H}}) \triangleq \mathbb{P}\big(\hat{\boldsymbol{H}}[1] = \hat{\mathbf{H}}\big)$$

the probability mass function of the quantized channel gains

$$\hat{\boldsymbol{H}}[t] \triangleq (\hat{h}_{m,k}[t])_{m,k}.$$

Note that the number of quantization regions is

$$|\hat{\mathcal{H}}| = \nu^4 L + 1. \tag{2}$$

By choosing ν large enough, we can ensure that the distance between any point with magnitude less than ν and its closest quantization point is arbitrarily small. In fact, for any $h_{m,k}[t]$ with $|h_{m,k}[t]| \leq \nu$,

$$|h_{m,k}[t] - \hat{h}_{m,k}[t]| \leq (\pi+1)/\nu. \tag{3}$$

Furthermore, for any $\delta > 0$,

$$\mathbb{P}\big(|h_{m,k}[t]| \leq \nu \ \forall m,k\big) \geq 1-\delta$$

for large enough ν by bounded convergence, and hence

$$\mathbb{P}\big(|\hat{h}_{m,k}[t]| < \infty \ \forall m,k\big) \geq 1-\delta. \tag{4}$$

Therefore (3) holds with probability at least $1-\delta$ for ν large enough. Finally, for any $h_{m,k}[t]$ such that $|h_{m,k}[t]| \leq \nu$,

$$\max\big\{|\hat{h}_{m,k}[t]|, |\hat{h}_{m,k}[t]|^{-1}\big\} \leq 2\max\big\{|h_{m,k}[t]|, |h_{m,k}[t]|^{-1}\big\}, \tag{5}$$

since each finite quantization point is the mid-point of the corresponding bisector interval.

Since the matrix process

$$\boldsymbol{H}[1], \boldsymbol{H}[2], \boldsymbol{H}[3], \dots$$

is stationary and ergodic, the quantized process

$$\hat{\boldsymbol{H}}[1], \hat{\boldsymbol{H}}[2], \hat{\boldsymbol{H}}[3], \dots$$

is also stationary and ergodic (see, e.g., [39, Theorem 6.1.1, Theorem 6.1.3]). Moreover, since each $h_{m,k}[t]$ is circularly symmetric, and since the quantization procedure preserves this circular symmetry, the distribution of the quantized channel values $\hat{h}_{m,k}[t]$ is invariant under multiplication by the Lth root of unity. Furthermore, since the K^2 processes $(h_{m,k}[t])_{t\in\mathbb{N}}$ are mutually independent as a function of m,k, so are the K^2 quantized processes $(\hat{h}_{m,k}[t])_{t\in\mathbb{N}}$. For future reference, we summarize these observations in the following lemma.

Lemma 3. *For each m,k, and t, the quantized channel gain $\hat{h}_{m,k}[t]$ and its rotation $\exp\big(\sqrt{-1}\frac{2\pi}{L}\big)\hat{h}_{m,k}[t]$ have the same distribution. The K^2 quantized processes*

$$\hat{h}_{m,k}[1], \hat{h}_{m,k}[2], \hat{h}_{m,k}[3], \dots$$

are independent as a function of m,k. The quantized matrix process

$$\hat{\boldsymbol{H}}[1], \hat{\boldsymbol{H}}[2], \hat{\boldsymbol{H}}[3], \dots$$

is stationary and ergodic.

We consider a block of length T of channel gains with T a multiple of L, and we divide this block into L subblocks each of length T/L. Count the number of occurrences of a particular channel realization $\hat{\mathsf{H}} \in \hat{\mathcal{H}}^{K\times K}$ in one of the L subblocks. By the ergodicity of the quantized matrix process, we expect this number to be close to T/L times the probability of this realization. The next lemma formalizes this statement.

Lemma 4. *For any $L,\nu \in \mathbb{N}$ and $\eta,\varepsilon > 0$, there exists $T = T(L,\nu) \in \mathbb{N}$ divisible by L such that, with probability at least $1-\varepsilon$, we have, for all $\ell \in \{1,\dots,L\}$, and all $\hat{\mathsf{H}} \in \hat{\mathcal{H}}^{K\times K}$,*

$$\sum_{t=(\ell-1)T/L+1}^{\ell T/L} \mathbb{1}\{\hat{\boldsymbol{H}}[t] = \hat{\mathsf{H}}\} \geq (1-\eta)p_{\hat{\boldsymbol{H}}}(\hat{\mathsf{H}})T/L.$$

Proof: By Lemma 3, the quantized matrix process

$$\hat{\boldsymbol{H}}[1], \hat{\boldsymbol{H}}[2], \hat{\boldsymbol{H}}[3], \dots$$

is stationary and ergodic. This stochastic process takes values in the finite set $\hat{\mathcal{H}}^{K\times K}$, and hence, by the ergodic theorem (see, e.g., [39, Theorem 6.2.1]), its empirical distribution converges to the true distribution almost surely. For fixed $\ell \in \{1, \dots, L\}$, this implies that there exists a T such that with probability at least $1 - \varepsilon/L$, we have for all $\hat{\mathsf{H}} \in \hat{\mathcal{H}}^{K\times K}$,

$$\sum_{t=(\ell-1)T/L+1}^{\ell T/L} \mathbb{1}\{\hat{\boldsymbol{H}}[t] = \hat{\mathsf{H}}\} \geq (1-\eta) p_{\hat{\boldsymbol{H}}}(\hat{\mathsf{H}}) T/L.$$

Applying the union bound over $\ell \in \{1, \dots, L\}$ proves the result. ■

V. PROOF OF LOWER BOUND IN THEOREM 1 FOR TWO USERS

In this section, we prove the lower bound in Theorem 1 for the two user case, i.e., $K = 2$. Consider a block of T channel gains, and divide this block into L subblocks each of length of T/L (assumed to be an integer). The construction of the achievable scheme in Theorem 1 consists of three main steps. First, we carefully match L time slots, one from each of the L subblocks. This matching is performed approximately T/L many times such that essentially all time slots in the block of length T are matched (see Section V-A). Second, we argue that any L time slots matched in this fashion, when considered jointly, can be transformed into a channel with (nearly) integer channel gains using appropriate linear precoders at the transmitters and matched filters at the receivers (see Section V-B). Third, we show that over this integer channel we can efficiently and reliably compute functions of the messages (see Section V-C).

A. *Matching of Channel Gains*

We start with the matching step. Since the number of possible channel realizations is uncountable, only approximate matching is possible. To this end, we quantize each of the channel gains as described in Section IV. Denote by $\hat{h}_{m,k}[t]$ the quantized version of the channel gain $h_{m,k}[t]$. By Lemma 4, for every $\varepsilon_1 > 0$ and $\eta > 0$, there exists T large enough such that with probability $1 - \varepsilon_1$, each of the L subblocks is "typical", in the sense that, for every subblock $\ell \in \{1, \dots, L\}$, and every realization $\hat{\mathsf{H}} \in \hat{\mathcal{H}}^{K\times K}$ of the quantized channel gains,

$$\sum_{t=(\ell-1)T/L+1}^{\ell T/L} \mathbb{1}\{\hat{\boldsymbol{H}}[t] = \hat{\mathsf{H}}\} \geq (1-\eta) p_{\hat{\boldsymbol{H}}}(\hat{\mathsf{H}}) T/L.$$

Recall that full CSI is available at all transmitters and receivers. Hence all transmitters and receivers can determine at the end of the block of length T if the realization of quantized channel gains is typical. Whenever this is not the case, the decoders declare an error. By the argument in the last paragraph, this happens with probability at most ε_1. We assume in the following discussion that the quantized channel gains are typical.

We can then assume that every matrix of quantized channel gains $\hat{\mathsf{H}}$ appears exactly[1]

$$(1-\eta) p_{\hat{\boldsymbol{H}}}(\hat{\mathsf{H}}) T/L \tag{6}$$

many times in each of the L blocks, ignoring all the remaining time slots. This results in a loss of at most a factor $(1-\eta)$ in rate. Furthermore, by the full CSI assumption, all receivers and transmitters can reorder the time slots within each of the L subblocks, and hence we may assume without loss of generality that the first $(1-\eta)T/L$ quantized channel gains in each subblock satisfy this condition.

---

[1] Since T/L will grow to infinity, we can assume here that (6) is integer and avoid floor operators.

We now describe the matching procedure alluded to earlier. Consider the channel gains at time $t_1 = 1$ in the first of the L subblocks and the corresponding matrix of quantized channel gains $\hat{\boldsymbol{H}}[t_1]$. Let t_ℓ be the first time in block $\ell \in \{2, \cdots, L\}$ such that

$$\hat{h}_{1,1}[t_\ell] = \hat{h}_{1,1}[t_1], \tag{7a}$$

$$\hat{h}_{1,2}[t_\ell] = \hat{h}_{1,2}[t_1], \tag{7b}$$

$$\hat{h}_{2,2}[t_\ell] = \hat{h}_{2,2}[t_1], \tag{7c}$$

$$\hat{h}_{2,1}[t_\ell] = \omega_L^{\ell-1}\hat{h}_{2,1}[t_1], \tag{7d}$$

where

$$\omega_L \triangleq \exp\left(\sqrt{-1}\tfrac{2\pi}{L}\right)$$

is the Lth root of unity. By construction of the quantization scheme, if $\hat{h} \in \hat{\mathcal{H}}$ then $\omega_L^{\ell-1}\hat{h} \in \hat{\mathcal{H}}$, and hence such a collection of time slots $t_2, \dots, t_L$ can exist. Since $t_1 < t_2 < \cdots < t_L$, this matching procedure can be performed in a causal manner. Moreover, by the full CSI assumption, this matching can be computed at each transmitter and receiver.

Having performed the matching for $t_1 = 1$, we proceed with $t_1 = 2$. We again match channel gains in the same fashion, ensuring that each time slot t_ℓ in subblocks $\ell \in \{2, \dots, L\}$ is chosen at most once. In other words, this matching procedure constructs many nonintersecting L-element subsets $\{t_1, \dots, t_L\}$ of $\{1, \dots, T\}$. We now argue that this procedure can be continued successfully up to $t_1 = (1-\eta)T/L$, i.e., $(1-\eta)T/L$ of these subsets can be found.

Consider a time slot t_1 in the first subblock and the corresponding channel gains $\hat{\boldsymbol{H}}[t_1]$. This channel gain induces matched channel gains

$$\hat{\boldsymbol{H}}[t_2], \hat{\boldsymbol{H}}[t_3], \dots, \hat{\boldsymbol{H}}[t_L],$$

within subblocks $2, \dots, L$. Hence, the distribution of the channel gains $\hat{\boldsymbol{H}}[t_1]$ at some fixed t_1 induces a distribution of the channel gains $\hat{\boldsymbol{H}}[t_\ell]$ for $\ell \in \{2, \dots, L\}$. It is not clear *a priori* that $\hat{\boldsymbol{H}}[t_\ell]$ and $\hat{\boldsymbol{H}}[t]$ for any fixed t have the same distribution.

The key observation for the analysis of the matching procedure is the following: By (6), the matching procedure is successful for all $t_1 \in \{1, \dots, (1-\eta)T/L\}$ if the distribution of $\hat{\boldsymbol{H}}[t_\ell]$ for $\ell \in \{2 \dots, L\}$ is the same as the distribution of $\hat{\boldsymbol{H}}[(\ell-1)T/L+1]$ (or any other channel matrix at *fixed* time t in subblock ℓ). By stationarity, the distribution of $\hat{\boldsymbol{H}}[(\ell-1)T/L+1]$ is the same as the distribution of $\hat{\boldsymbol{H}}[1]$. Hence, it suffices to argue that $\hat{\boldsymbol{H}}[t_\ell]$ has the same distribution as $\hat{\boldsymbol{H}}[1]$, i.e., that $\hat{\boldsymbol{H}}[t_\ell]$ has distribution $p_{\hat{\boldsymbol{H}}}$. We now show that this is the case.

By assumption, the distribution of each channel gain $h_{m,k}[t]$ is circularly symmetric. By Lemma 3, the quantization scheme preserves this circular symmetry, in the sense that all possible quantized channel gains with the same magnitude have the same probability. Since the components of $\hat{\boldsymbol{H}}[t]$ are independent by Lemma 3, this circular symmetry also holds for their joint distribution, i.e., if $\hat{\mathsf{H}}$ and $\hat{\mathsf{H}}'$ satisfy $|\hat{\mathsf{h}}_{m,k}| = |\hat{\mathsf{h}}'_{m,k}|$ for all m, k, then

$$p_{\hat{\boldsymbol{H}}}(\hat{\mathsf{H}}') = p_{\hat{\boldsymbol{H}}}(\hat{\mathsf{H}}).$$

Observe now that, for each m, k, the channel gains

$$\hat{h}_{m,k}[t_1], \hat{h}_{m,k}[t_2], \dots, \hat{h}_{m,k}[t_L],$$

all have the same magnitude by the matching condition (7). Moreover, since the distribution of $\hat{\boldsymbol{H}}[t_1]$ is circularly symmetric, and since (7) results in a *fixed* phase shift, the induced distribution of the matched channel gains $\hat{\boldsymbol{H}}[t_\ell]$ is circularly symmetric as well. Together, these two facts shows that the distribution of the quantized channel gains induced by the matching within the subblocks $\ell \in \{2, \dots, L\}$ is identical to the distribution of the quantized channel gains within the first subblock. This implies that the time slots $t_1 = 1$ up to $t_1 = (1-\eta)T/L$ can be matched up by the described procedure.

Out of the $(1-\eta)T/L$ time slots that are matched in this fashion, at most $\delta(1-\eta)T/L$ contain a quantized channel gain equal to infinity by (4) for some $\delta=\delta(\nu)$ (where ν is the parameter governing the number of quantization points). These time slots are not used. Again by the full CSI assumption, this event can be observed at each transmitter and receiver. Accounting for the time slots that are not matched, a total of at least $(1-\eta)(1-\delta)T/L$ time slots in each subblock are used for communication.

To summarize, the channel gains in each of the L subblocks are matched up to satisfy (7). With probability at least

$$1-\varepsilon_1(T), \tag{8}$$

at least a fraction

$$(1-\eta(T))(1-\delta(\nu))$$

of the time slots in each subblock can be matched in this fashion such that all the corresponding channel gains have finite magnitudes. Here the parameters can be chosen to satisfy

$$\lim_{T\to\infty}\varepsilon_1(T)=0, \tag{9}$$

$$\lim_{T\to\infty}\eta(T)=0, \tag{10}$$

both for fixed values of L and ν, and

$$\lim_{\nu\to\infty}\delta(\nu)=0. \tag{11}$$

B. Precoding and Matched Filtering

Consider time slots $t_1,\dots,t_L$ in subblocks $1,\dots,L$ that are matched as described in the last section. We now describe a linear precoding transmitter design and matched filtering receiver design that transform the complex channel over these L time slots into an integer channel.

Construct the diagonal matrix

$$\boldsymbol{D}_{m,k}\triangleq\operatorname{diag}\big((h_{m,k}[t_\ell])_{\ell=1}^{L}\big),$$

from the L matched channel gains between transmitter k and receiver m and define $\hat{\boldsymbol{D}}_{m,k}$ in the same manner, but with respect to $\hat{h}_{m,k}[t_\ell]$. Observe from (7) that

$$\hat{\boldsymbol{D}}_{m,k}=\begin{cases}\hat{h}_{m,k}\boldsymbol{I} & \text{if } (m,k)\neq(2,1),\\ \hat{h}_{m,k}\boldsymbol{F} & \text{if } (m,k)=(2,1)\end{cases}$$

by the matching procedure, where

$$\hat{h}_{m,k}\triangleq\hat{h}_{m,k}[t_1],$$

and

$$\boldsymbol{F}\triangleq\operatorname{diag}\big((\omega_L^{\ell-1})_{\ell=1}^{L}\big).$$

Each transmitter uses a linear precoder over the block of L symbols. In other words, each message symbol is multiplied by a transmit vector in $\mathbb{C}^L$. The modulated transmit vectors are summed up by the transmitter. At time t_ℓ, the component ℓ of this sum of vectors is sent over the channel.

Transmitter one uses a total of L transmit vectors. The first transmit vector is

$$\boldsymbol{v}_{1,1}\triangleq\boldsymbol{1},$$

where $\boldsymbol{1}$ denotes the vector of all ones. The remaining transmit vectors $\boldsymbol{v}_{1,\ell}$ for $\ell\in\{2,\dots,L\}$ are obtained recursively as

$$\boldsymbol{v}_{1,\ell}\triangleq b_\ell\hat{\boldsymbol{D}}_{2,1}^{-1}\hat{\boldsymbol{D}}_{2,2}\hat{\boldsymbol{D}}_{1,2}^{-1}\hat{\boldsymbol{D}}_{1,1}\boldsymbol{v}_{1,\ell-1}=b_\ell\frac{\hat{h}_{2,2}\hat{h}_{1,1}}{\hat{h}_{2,1}\hat{h}_{1,2}}\boldsymbol{F}^{-1}\boldsymbol{v}_{1,\ell-1},$$

where the scalar b_ℓ is of the form n or $1/n$ for the smallest natural number $n \in \mathbb{N}$ such that

$$\|\boldsymbol{v}_{1,\ell}\|/\sqrt{L} \in [1,2). \tag{12}$$

For convenience of notation, we set $b_1 \triangleq 1$. The scalar b_ℓ can be interpreted as a normalization constant; it ensures that all transmit vectors have approximately the same norm. The reason that b_ℓ has to be a small integer or its inverse will become clear later.

Transmitter two uses a total of $L-1$ transmit vectors, which are defined through the transmit vectors for transmitter one. Transmit vector $\boldsymbol{v}_{2,\ell}$ for $\ell \in \{1,\dots,L-1\}$ is

$$\boldsymbol{v}_{2,\ell} \triangleq \hat{\boldsymbol{D}}_{1,2}^{-1}\hat{\boldsymbol{D}}_{1,1}\boldsymbol{v}_{1,\ell} = \frac{\hat{h}_{1,1}}{\hat{h}_{1,2}}\boldsymbol{v}_{1,\ell}.$$

Define

$$c = c(\hat{\boldsymbol{H}}) \triangleq \prod_{m,k} \max\big\{|\hat{h}_{m,k}|, |\hat{h}_{m,k}|^{-1}\big\}. \tag{13}$$

It follows from (12) that

$$1/c \le \frac{|\hat{h}_{1,1}|}{|\hat{h}_{1,2}|} \le \|\boldsymbol{v}_{2,\ell}\|/\sqrt{L} \le 2\frac{|\hat{h}_{1,1}|}{|\hat{h}_{1,2}|} \le 2c \tag{14}$$

and that

$$\max\{b_\ell, b_\ell^{-1}\} \le 2c. \tag{15}$$

Observe that every transmit vector $\boldsymbol{v}_{k,\ell}$ is of the form

$$\boldsymbol{v}_{k,\ell} = \rho \boldsymbol{F}^{\alpha}\mathbf{1}$$

for some scalars $\rho \in \mathbb{C}$ and $\alpha \in \mathbb{N}$. Since

$$\mathbf{1}^{\mathsf{T}}\boldsymbol{F}^{\alpha}\mathbf{1} = \mathbb{1}_{\{\alpha \in L\mathbb{Z}\}}, \tag{16}$$

this ensures that two different transmit vectors are either collinear or orthogonal.

Each transmitter modulates independent message symbols over its transmit vectors. We will provide a detailed description as to how these symbols constitute codewords across matchings of time slots in Section V-C. Transmitter one has access to L symbols $s_{1,1},\dots,s_{1,L}$ and transmitter two has access to $L-1$ symbols $s_{2,1},\dots,s_{2,L-1}$. We assume that all these $2L-1$ symbols have zero mean and are mutually independent.

The vector of channel inputs

$$\boldsymbol{x}_k \triangleq \begin{pmatrix} x_k[t_1] & x_k[t_2] & \cdots & x_k[t_L] \end{pmatrix}^{\mathsf{T}}$$

at time slots $t_1,\dots,t_L$ at transmitter $k \in \{1,2\}$ is given by

$$\boldsymbol{x}_1 = \sum_{\ell=1}^{L} s_{1,\ell}\boldsymbol{v}_{1,\ell},$$

and

$$\boldsymbol{x}_2 = \sum_{\ell=1}^{L-1} s_{2,\ell}\boldsymbol{v}_{2,\ell}.$$

We allocate the same amount of power

$$\mathbb{E}\big(|s_{k,\ell}|^2\big) = \frac{P}{4Lc^2} \triangleq \tilde{P} \tag{17}$$

to each $s_{k,\ell}$. Since $\|\boldsymbol{v}_{k,\ell}\|^2 \leq 4Lc^2$ by (12) and (14), we have

$$\frac{1}{L}\mathbb{E}\big(\|\boldsymbol{x}_k\|^2\big) \leq P,$$

satisfying the overall average power constraint of P over the L time slots $t_1, \dots, t_L$. Since transmitter one has L transmit vectors and transmitter two has $L-1$ transmit vectors, the transmitters send a total of $2L-1$ data streams over L channel uses.

The vector

$$\boldsymbol{y}_m \triangleq \begin{pmatrix} y_m[t_1] & y_m[t_2] & \cdots & y_m[t_L] \end{pmatrix}^{\mathsf{T}}$$

of channel outputs at time slots $t_1, \dots, t_L$ at receiver m is then

$$\begin{aligned} \boldsymbol{y}_m &= \boldsymbol{D}_{m,1}\boldsymbol{x}_1 + \boldsymbol{D}_{m,2}\boldsymbol{x}_2 + \boldsymbol{z}_m \\ &= \sum_{\ell=1}^{L} s_{1,\ell}\boldsymbol{D}_{m,1}\boldsymbol{v}_{1,\ell} + \sum_{\ell=1}^{L-1} s_{2,\ell}\boldsymbol{D}_{m,2}\boldsymbol{v}_{2,\ell} + \boldsymbol{z}_m, \end{aligned} \tag{18}$$

where

$$\boldsymbol{z}_m \triangleq \begin{pmatrix} z_m[t_1] & z_m[t_2] & \cdots & z_m[t_L] \end{pmatrix}^{\mathsf{T}}$$

is the additive noise at receiver m.

Each receiver $m \in \{1, 2\}$ uses matched filters on the received channel outputs $\boldsymbol{y}_m$, which we describe next. Assume for the moment that the channel gains $\boldsymbol{D}_{m,k}$ are equal to their quantized version $\hat{\boldsymbol{D}}_{m,k}$. Consider two transmit vectors $\boldsymbol{v}_{1,\ell}$ and $\boldsymbol{v}_{2,\ell}$. At receiver one, these transmit vectors are observed as

$$\hat{\boldsymbol{D}}_{1,1}\boldsymbol{v}_{1,\ell} = \hat{h}_{1,1}\boldsymbol{v}_{1,\ell}, \tag{19a}$$

and

$$\hat{\boldsymbol{D}}_{1,2}\boldsymbol{v}_{2,\ell} = \hat{\boldsymbol{D}}_{1,2}\frac{\hat{h}_{1,1}}{\hat{h}_{1,2}}\boldsymbol{v}_{1,\ell} = \hat{h}_{1,1}\boldsymbol{v}_{1,\ell}. \tag{19b}$$

Hence the two transmit vectors $\boldsymbol{v}_{1,\ell}$ and $\boldsymbol{v}_{2,\ell}$ are *aligned* at receiver one. Similarly, the two transmit vectors $\boldsymbol{v}_{1,\ell+1}$ and $\boldsymbol{v}_{2,\ell}$ are observed at receiver two as

$$\hat{\boldsymbol{D}}_{2,1}\boldsymbol{v}_{1,\ell+1} = b_{\ell+1}\hat{\boldsymbol{D}}_{2,2}\hat{\boldsymbol{D}}_{1,2}^{-1}\hat{\boldsymbol{D}}_{1,1}\boldsymbol{v}_{1,\ell} = b_{\ell+1}\hat{h}_{2,2}\boldsymbol{v}_{2,\ell}, \tag{20a}$$

and

$$\hat{\boldsymbol{D}}_{2,2}\boldsymbol{v}_{2,\ell} = \hat{h}_{2,2}\boldsymbol{v}_{2,\ell}. \tag{20b}$$

Again, the two transmit vectors $\boldsymbol{v}_{1,\ell+1}$ and $\boldsymbol{v}_{2,\ell}$ are aligned at receiver two. Moreover, all other transmit vectors are received in orthogonal directions at both receivers by (16), since they have a different power of the diagonal "Fourier" matrix $\boldsymbol{F}$. Thus each receiver observes a linear combination of L orthogonal vectors with $L-1$ of these vectors carrying an aligned message symbol from both transmitter one and transmitter two. This situation is illustrated for $L = 2$ in Fig. 3 in Section III-A.

Thus, if $\boldsymbol{D}_{m,k} = \hat{\boldsymbol{D}}_{m,k}$ for all $m, k \in \{1, 2\}$, then each receiver can project the received signal onto the L rotated transmit vectors. For one of these vectors, there is just one transmitted signal. For the remaining $L-1$ observed vectors, the receiver must decode the sum of the two aligned data streams. Formally, this operation of the receivers is implemented by multiplying the vector of channel outputs $\boldsymbol{y}_m$ by the matched filter

$$\tilde{\boldsymbol{v}}_{m,j} \triangleq \boldsymbol{v}_{m,j}/\|\boldsymbol{v}_{m,j}\|$$

for $m = 1, j \in \{1, \dots, L\}$ and for $m = 2, j \in \{1, \dots, L-1\}$, to form

$$\tilde{\boldsymbol{v}}_{m,j}^{\dagger}\boldsymbol{y}_m.$$

In general, the channel gains are not equal to their quantized versions, i.e., $\boldsymbol{D}_{m,k} \neq \hat{\boldsymbol{D}}_{m,k}$. However, since we only communicate during time slots satisfying $|h_{m,k}[t]| \leq \nu$, the quantization error is upper bounded by (3) as

$$|h_{m,k}[t_\ell] - \hat{h}_{m,k}[t_\ell]| \leq (\pi + 1)/\nu,$$

so the matrices $\boldsymbol{D}_{m,k}$ and $\hat{\boldsymbol{D}}_{m,k}$ are quite close for quantization parameter ν large enough. We will use the same receiver structure as for the perfectly matched case, i.e., we use the matched filters according to the quantized matrices. To determine performance, we will bound the additional interference that is caused by imperfect alignment (received vectors do not line up) and imperfect zero forcing of interference (received vectors are not orthogonal).

Using (18), the output of the jth matched filter $\tilde{\boldsymbol{v}}_{m,j}$ at receiver m is then

$$\tilde{\boldsymbol{v}}_{m,j}^\dagger \boldsymbol{y}_m = \sum_{\ell=1}^{L} s_{1,\ell} \tilde{\boldsymbol{v}}_{m,j}^\dagger \boldsymbol{D}_{m,1} \boldsymbol{v}_{1,\ell} + \sum_{\ell=1}^{L-1} s_{2,\ell} \tilde{\boldsymbol{v}}_{m,j}^\dagger \boldsymbol{D}_{m,2} \boldsymbol{v}_{2,\ell} + \tilde{\boldsymbol{v}}_{m,j}^\dagger \boldsymbol{z}_m.$$

Defining

$$\boldsymbol{\Upsilon}_{m,k} \triangleq \boldsymbol{D}_{m,k} - \hat{\boldsymbol{D}}_{m,k}$$

as the (diagonal) matrix of channel quantization errors, we can rewrite the output of the matched filter at receiver one

$$\begin{aligned}\tilde{\boldsymbol{v}}_{1,j}^\dagger \boldsymbol{y}_1 = {} & s_{1,j} \tilde{\boldsymbol{v}}_{1,j}^\dagger \hat{\boldsymbol{D}}_{1,1} \boldsymbol{v}_{1,j} + s_{2,j} \tilde{\boldsymbol{v}}_{1,j}^\dagger \hat{\boldsymbol{D}}_{1,2} \boldsymbol{v}_{2,j} \\ & + s_{1,j} \tilde{\boldsymbol{v}}_{1,j}^\dagger \boldsymbol{\Upsilon}_{1,1} \boldsymbol{v}_{1,j} + s_{2,j} \tilde{\boldsymbol{v}}_{1,j}^\dagger \boldsymbol{\Upsilon}_{1,2} \boldsymbol{v}_{2,j} + \textstyle\sum_{\ell \neq j} s_{1,\ell} \tilde{\boldsymbol{v}}_{1,j}^\dagger \boldsymbol{D}_{1,1} \boldsymbol{v}_{1,\ell} + \textstyle\sum_{\ell \neq j} s_{2,\ell} \tilde{\boldsymbol{v}}_{1,j}^\dagger \boldsymbol{D}_{1,2} \boldsymbol{v}_{2,\ell} \\ & + \tilde{\boldsymbol{v}}_{1,j}^\dagger \boldsymbol{z}_1 \end{aligned} \tag{21a}$$

for $j \in \{1, \dots, L-1\}$ and

$$\begin{aligned}\tilde{\boldsymbol{v}}_{1,L}^\dagger \boldsymbol{y}_1 = {} & s_{1,L} \tilde{\boldsymbol{v}}_{1,L}^\dagger \hat{\boldsymbol{D}}_{1,1} \boldsymbol{v}_{1,L} \\ & + s_{1,L} \tilde{\boldsymbol{v}}_{1,L}^\dagger \boldsymbol{\Upsilon}_{1,1} \boldsymbol{v}_{1,L} + \textstyle\sum_{\ell=1}^{L-1} s_{1,\ell} \tilde{\boldsymbol{v}}_{1,L}^\dagger \boldsymbol{D}_{1,1} \boldsymbol{v}_{1,\ell} + \textstyle\sum_{\ell=1}^{L-1} s_{2,\ell} \tilde{\boldsymbol{v}}_{1,L}^\dagger \boldsymbol{D}_{1,2} \boldsymbol{v}_{2,\ell} \\ & + \tilde{\boldsymbol{v}}_{1,L}^\dagger \boldsymbol{z}_1 \end{aligned} \tag{21b}$$

for $j = L$. Similarly, we can rewrite the output of the matched filter at receiver two as

$$\begin{aligned}\tilde{\boldsymbol{v}}_{2,j}^\dagger \boldsymbol{y}_2 = {} & s_{1,j+1} \tilde{\boldsymbol{v}}_{2,j}^\dagger \hat{\boldsymbol{D}}_{2,1} \boldsymbol{v}_{1,j+1} + s_{2,j} \tilde{\boldsymbol{v}}_{2,j}^\dagger \hat{\boldsymbol{D}}_{2,2} \boldsymbol{v}_{2,j} \\ & + s_{1,j+1} \tilde{\boldsymbol{v}}_{2,j}^\dagger \boldsymbol{\Upsilon}_{2,1} \boldsymbol{v}_{1,j+1} + s_{2,j} \tilde{\boldsymbol{v}}_{2,j}^\dagger \boldsymbol{\Upsilon}_{2,2} \boldsymbol{v}_{2,j} + \textstyle\sum_{\ell \neq j+1} s_{1,\ell} \tilde{\boldsymbol{v}}_{2,j}^\dagger \boldsymbol{D}_{2,1} \boldsymbol{v}_{1,\ell} + \textstyle\sum_{\ell \neq j} s_{2,\ell} \tilde{\boldsymbol{v}}_{2,j}^\dagger \boldsymbol{D}_{2,2} \boldsymbol{v}_{2,\ell} \\ & + \tilde{\boldsymbol{v}}_{2,j}^\dagger \boldsymbol{z}_2 \end{aligned} \tag{21c}$$

for $j \in \{1, \dots, L-1\}$. From (21), we see that the matched filter output consists of three parts: desired signal, mismatch terms due to imperfect alignment and imperfect zero forcing of interference, and receiver noise.

We start with the analysis of the desired signals in (21). The desired signal at receiver one is

$$s_{1,j} \tilde{\boldsymbol{v}}_{1,j}^\dagger \hat{\boldsymbol{D}}_{1,1} \boldsymbol{v}_{1,j} + s_{2,j} \tilde{\boldsymbol{v}}_{1,j}^\dagger \hat{\boldsymbol{D}}_{1,2} \boldsymbol{v}_{2,j} = \hat{h}_{1,1} \|\boldsymbol{v}_{1,j}\| (s_{1,j} + s_{2,j}) \tag{22a}$$

for $j \in \{1, \dots, L-1\}$ and

$$s_{1,L} \tilde{\boldsymbol{v}}_{1,L}^\dagger \hat{\boldsymbol{D}}_{1,1} \boldsymbol{v}_{1,L} = \hat{h}_{1,1} \|\boldsymbol{v}_{1,L}\| s_{1,L} \tag{22b}$$

for $j = L$, where we have used (19). Similarly, the desired signal at receiver two is

$$s_{1,j+1} \tilde{\boldsymbol{v}}_{2,j}^\dagger \hat{\boldsymbol{D}}_{2,1} \boldsymbol{v}_{1,j+1} + s_{2,j} \tilde{\boldsymbol{v}}_{2,j}^\dagger \hat{\boldsymbol{D}}_{2,2} \boldsymbol{v}_{2,j} = \hat{h}_{2,2} \|\boldsymbol{v}_{2,j}\| (b_{j+1} s_{1,j+1} + s_{2,j}) \tag{22c}$$

for $j \in \{1, \dots, L-1\}$, where we have used (20). Using (12), (13), (14), and (17), the received signal power (for each symbol) satisfies

$$|\hat{h}_{1,1}|^2 \|\boldsymbol{v}_{1,j}\|^2 \mathbb{E}\big(|s_{k,j}|^2\big) \geq |\hat{h}_{1,1}|^2 L\tilde{P} \geq \frac{L\tilde{P}}{c^2}. \tag{23a}$$

at receiver one and

$$|\hat{h}_{2,2}|^2 \|\boldsymbol{v}_{2,j}\|^2 \mathbb{E}\big(|s_{k,j}|^2\big) \geq \frac{|\hat{h}_{2,2}|^2 |\hat{h}_{1,1}|^2}{|\hat{h}_{1,2}|^2} L\tilde{P} \geq \frac{L\tilde{P}}{c^2} \tag{23b}$$

at receiver two (not accounting for the normalization factor b_{j+1}).

Before we continue with the analysis of the mismatch terms in (21), we argue that $|\tilde{\boldsymbol{v}}_{m,j}^\dagger \boldsymbol{\Upsilon}_{m,k} \boldsymbol{v}_{k,\ell}|^2$ is small. By the Cauchy-Schwarz inequality,

$$|\tilde{\boldsymbol{v}}_{m,j}^\dagger \boldsymbol{\Upsilon}_{m,k} \boldsymbol{v}_{k,\ell}|^2 \leq \|\tilde{\boldsymbol{v}}_{m,j}\|^2 \|\boldsymbol{\Upsilon}_{m,k}\|^2 \|\boldsymbol{v}_{k,\ell}\|^2, \tag{24}$$

where $\|\boldsymbol{\Upsilon}_{m,k}\|^2$ denotes the sum of squared diagonal entries of $\boldsymbol{\Upsilon}_{m,k}$. By construction, $\|\tilde{\boldsymbol{v}}_{k,j}\|^2 = 1$. From (3), $\|\boldsymbol{\Upsilon}_{m,k}\|^2$ satisfies

$$\|\boldsymbol{\Upsilon}_{m,k}\|^2 \leq L(\pi+1)^2/\nu^2.$$

By (12) and (14),

$$\|\boldsymbol{v}_{k,j}\|^2 \leq 4Lc^2$$

for $k \in \{1,2\}$, where we have used that $c \geq 1$ by (13). Combining this with (24) yields the desired upper bound

$$|\tilde{\boldsymbol{v}}_{m,j}^\dagger \boldsymbol{\Upsilon}_{m,k} \boldsymbol{v}_{k,\ell}|^2 \leq \frac{4L^2(\pi+1)^2 c^2}{\nu^2} \triangleq \gamma^2. \tag{25}$$

The mismatch term in (21) due to imperfect alignment is

$$s_{1,j} \tilde{\boldsymbol{v}}_{1,j}^\dagger \boldsymbol{\Upsilon}_{1,1} \boldsymbol{v}_{1,j} + s_{2,j} \tilde{\boldsymbol{v}}_{1,j}^\dagger \boldsymbol{\Upsilon}_{1,2} \boldsymbol{v}_{2,j} \triangleq e_{1,1,j} s_{1,j} + e_{1,2,j} s_{2,j} \tag{26a}$$

at receiver one, and

$$s_{1,j+1} \tilde{\boldsymbol{v}}_{2,j}^\dagger \boldsymbol{\Upsilon}_{2,1} \boldsymbol{v}_{1,j+1} + s_{2,j} \tilde{\boldsymbol{v}}_{2,j}^\dagger \boldsymbol{\Upsilon}_{2,2} \boldsymbol{v}_{2,j} \triangleq e_{2,1,j} s_{1,j+1} + e_{2,2,j} s_{2,j} \tag{26b}$$

at receiver two. Each term $e_{m,k,j}$ can be interpreted as the residual channel fluctuation after the quantized matching, and satisfies

$$|e_{m,k,j}|^2 \leq \gamma^2 \tag{27}$$

by (25).

The mismatch term in (21) due to imperfect zero forcing is

$$\begin{aligned} \theta_{1,j} &\triangleq \sum_{\ell \neq j} s_{1,\ell} \tilde{\boldsymbol{v}}_{1,j}^\dagger \boldsymbol{D}_{1,1} \boldsymbol{v}_{1,\ell} + \sum_{\ell \neq j} s_{2,\ell} \tilde{\boldsymbol{v}}_{1,j}^\dagger \boldsymbol{D}_{1,2} \boldsymbol{v}_{2,\ell} \\ &= \sum_{\ell \neq j} s_{1,\ell} \tilde{\boldsymbol{v}}_{1,j}^\dagger \boldsymbol{\Upsilon}_{1,1} \boldsymbol{v}_{1,\ell} + \sum_{\ell \neq j} s_{2,\ell} \tilde{\boldsymbol{v}}_{1,j}^\dagger \boldsymbol{\Upsilon}_{1,2} \boldsymbol{v}_{2,\ell} \end{aligned} \tag{28a}$$

at receiver one, where we have used the orthogonality of the received vectors under channel gains $\hat{\boldsymbol{D}}_{m,k}$. Similarly,

$$\begin{aligned} \theta_{2,j} &\triangleq \sum_{\ell \neq j+1} s_{1,\ell} \tilde{\boldsymbol{v}}_{2,j}^\dagger \boldsymbol{D}_{2,1} \boldsymbol{v}_{2,\ell} + \sum_{\ell \neq j} s_{2,\ell} \tilde{\boldsymbol{v}}_{2,j}^\dagger \boldsymbol{D}_{2,2} \boldsymbol{v}_{2,\ell} \\ &= \sum_{\ell \neq j+1} s_{1,\ell} \tilde{\boldsymbol{v}}_{2,j}^\dagger \boldsymbol{\Upsilon}_{2,1} \boldsymbol{v}_{2,\ell} + \sum_{\ell \neq j} s_{2,\ell} \tilde{\boldsymbol{v}}_{2,j}^\dagger \boldsymbol{\Upsilon}_{2,2} \boldsymbol{v}_{2,\ell} \end{aligned} \tag{28b}$$

at receiver two. Using (17) and (25) together with the independence of the signals $s_{k,\ell}$, the total zero-forcing leakage power σ^2 is upper bounded by

$$\sigma^2 \triangleq \max_{m,j} \mathbb{E}\big(|\theta_{m,j}|^2\big) \leq 2(L-1)\gamma^2 \tilde{P} \tag{29}$$

at each receiver.

Finally, the additive noise term

$$\tilde{z}_{m,j} \triangleq \tilde{\boldsymbol{v}}_{m,j}^{\dagger} \boldsymbol{z}_m \tag{30}$$

in (21) is circularly-symmetric complex Gaussian with mean zero and variance one, since $\|\tilde{\boldsymbol{v}}_{m,j}\|^2 = 1$.

Substituting (22), (26), (28), and (30) into (21), yields that the output of the jth matched filter at receiver one is

$$\tilde{\boldsymbol{v}}_{1,j}^{\dagger} \boldsymbol{y}_1 = \begin{cases} \hat{h}_{1,1} \|\boldsymbol{v}_{1,j}\| (s_{1,j} + s_{2,j}) + \mu_{1,j} & j \neq L, \\ \hat{h}_{1,1} \|\boldsymbol{v}_{1,L}\| s_{1,L} + \mu_{1,L} & j = L, \end{cases} \tag{31}$$

where

$$\mu_{1,j} \triangleq \begin{cases} e_{1,1,j} s_{1,j} + e_{1,2,j} s_{2,j} + \theta_{1,j} + \tilde{z}_{1,j} & j \neq L, \\ e_{1,1,j} s_{1,j} + \theta_{1,j} + \tilde{z}_{1,j} & j = L, \end{cases} \tag{32}$$

is the sum of the imperfect alignment, imperfect zero forcing, and noise terms.[2] Using (17), (23), (27), (29), and (30), the signal-to-interference-and-noise ratio (SINR) for each subchannel at receiver one is lower bounded by

$$\begin{aligned} \mathsf{SINR}_1 &\geq \frac{L\tilde{P}/c^2}{1 + \sigma^2 + 2\gamma^2 \tilde{P}} \\ &\geq \frac{L\tilde{P}/c^2}{1 + 2L\gamma^2 \tilde{P}} \\ &= \frac{P/(4c^4)}{1 + 2L^2(\pi+1)^2 c^2 P/(\nu^2 c^2)} \\ &= \frac{P/(4c^4)}{1 + 2L^2(\pi+1)^2 P/\nu^2}. \end{aligned} \tag{33}$$

Similarly, at receiver two, we have

$$\tilde{\boldsymbol{v}}_{2,j}^{\dagger} \boldsymbol{y}_2 = \hat{h}_{2,2} \|\boldsymbol{v}_{2,j}\| (b_{j+1} s_{1,j+1} + s_{2,j}) + \mu_{2,j} \tag{34}$$

with

$$\mu_{2,j} \triangleq e_{2,1,j} s_{1,j+1} + e_{2,2,j} s_{2,j} + \theta_{2,j} + \tilde{z}_{2,j}. \tag{35}$$

Recall that b_{j+1} is of the form n or $1/n$ for some natural number $n \in \mathbb{N}$ with $n \leq 2c$ by (15). If $b_{j+1} = n$, then both channels have integer coefficients. If $b_{j+1} = 1/n$, then we can multiply the channel output by n to obtain a channel with integer coefficients. This decreases the effective SINR by at most a factor $4c^2$. Following the same steps as before, the signal-to-interference-and-noise ratio is lower bounded by

$$\mathsf{SINR}_2 \geq \frac{P/(16c^6)}{1 + 2L^2(\pi+1)^2 P/\nu^2}. \tag{36}$$

As we had seen earlier, the b_i factor serves as a normalizing term to ensure that all the transmit vectors $\boldsymbol{v}_{k,i}$ have approximately magnitude $\sqrt{L}$. From (34), it is now clear why b_j has to be chosen as a small integer or its inverse. Indeed, it is precisely this property that ensures that the subchannels induced by the matching of channel gains and the precoder / matched filter have essentially integer channel gains. As we will see, having integer channel gains significantly simplifies the task of efficient reliable computation. This transformation of the original channel with real coefficients into subchannels with integer coefficients is at the heart of the proposed communication scheme.

---

[2] The noise term $\mu_{1,j}$ depends on the signal $s_{k,\ell}$ and is, therefore, not additive. We will handle this difficulty later.

C. Computation of Functions

In the last section, we constructed and analyzed the channel induced by the linear precoder and matched filter. We now show how to reliably compute functions over this channel from the precoder input to the matched filter output.

Consider all time slots in the first subblock with quantized channel realization $\hat{\mathsf{H}} \in \hat{\mathcal{H}}^{K\times K}$. By Lemma 4, with probability at least $1-\varepsilon_1(T)$ there are at least

$$T^{(\hat{\mathsf{H}})} \triangleq (1-\eta(T))p_{\hat{\boldsymbol{H}}}(\hat{\mathsf{H}})T/L \tag{37}$$

time slots in the first subblock that have this quantized channel realization. By the matching construction in Section V-A, the first $T^{(\hat{\mathsf{H}})}$ such time slots can be successfully matched with time slots in subblocks $\ell \in \{2,\dots,L\}$ with quantized channel realizations chosen according to (7).

By (31) and (34), the precoding and matched filtering scheme from Section V-B, transform each group of L time slots into $L-1$ subchannels of the form

$$r_{1,j}^{(\hat{\mathsf{H}})}[t] = \beta_{1,j}^{(\hat{\mathsf{H}})}\big(s_{1,j}^{(\hat{\mathsf{H}})}[t] + s_{2,j}^{(\hat{\mathsf{H}})}[t]\big) + \mu_{1,j}^{(\hat{\mathsf{H}})}[t] \tag{38a}$$

$$r_{2,j}^{(\hat{\mathsf{H}})}[t] = \beta_{2,j}^{(\hat{\mathsf{H}})}\big(a_{1,j+1}^{(\hat{\mathsf{H}})}s_{1,j+1}^{(\hat{\mathsf{H}})}[t] + a_{2,j}^{(\hat{\mathsf{H}})}s_{2,j}^{(\hat{\mathsf{H}})}[t]\big) + \mu_{2,j}^{(\hat{\mathsf{H}})}[t] \tag{38b}$$

for $j \in \{1,\dots,L-1\}$, and where $s_{k,j}^{(\hat{\mathsf{H}})}$ are the channel inputs, $a_{1,j+1}^{(\hat{\mathsf{H}})}$ and $a_{2,j}^{(\hat{\mathsf{H}})}$ are nonzero integers, $\beta_{m,j}^{(\hat{\mathsf{H}})}$ are positive scaling factors, and $\mu_{1,j}^{(\hat{\mathsf{H}})}[t]$ and $\mu_{2,j}^{(\hat{\mathsf{H}})}[t]$ are interference and noise as in (32) and (35). Receiver one observes one additional subchannel of the form

$$r_{1,L}^{(\hat{\mathsf{H}})}[t] = \beta_{1,L}^{(\hat{\mathsf{H}})}s_{1,L}^{(\hat{\mathsf{H}})}[t] + \mu_{1,L}^{(\hat{\mathsf{H}})}[t]. \tag{38c}$$

From (33) and (36), the SINR to all of these subchannels is lower bounded by

$$\begin{aligned}\mathsf{SINR}(\hat{\mathsf{H}}) &\triangleq \min_m \mathsf{SINR}_m(\hat{\mathsf{H}}) \\ &\geq \frac{P/(16c^6(\hat{\mathsf{H}}))}{1+2L^2(\pi+1)^2P/\nu^2}.\end{aligned} \tag{39}$$

where we have explicitly written out the dependence of c and SINR on $\hat{\mathsf{H}}$.

Each transmitter k splits its message w_k into non-overlapping submessages $\boldsymbol{w}_{k,j}^{\hat{\mathsf{H}}}$, one for each subchannel j of quantized channel realization $\hat{\mathsf{H}}$. Each such submessage is a vector with components in $\{0,1,\dots,q-1\}$. Receiver one attempts to recover the functions

$$\boldsymbol{u}_{1,j}^{(\hat{\mathsf{H}})} \triangleq \begin{cases}\boldsymbol{w}_{1,j}^{(\hat{\mathsf{H}})} + \boldsymbol{w}_{2,j}^{(\hat{\mathsf{H}})} \pmod q & \text{if } j \in \{1,\dots,L-1\}, \\ \boldsymbol{w}_{1,L}^{(\hat{\mathsf{H}})} & \text{otherwise,}\end{cases}$$

over subchannel $j \in \{1,\dots,L\}$. Receiver two attempts to recover the functions

$$\boldsymbol{u}_{2,j}^{(\hat{\mathsf{H}})} \triangleq a_{1,j+1}^{(\hat{\mathsf{H}})}\boldsymbol{w}_{1,j+1}^{(\hat{\mathsf{H}})} + a_{2,j}^{(\hat{\mathsf{H}})}\boldsymbol{w}_{2,j}^{(\hat{\mathsf{H}})} \pmod q$$

over subchannel $j \in \{1,\dots,L-1\}$.

These equations are clearly invertible. Indeed, receiver one decodes $\boldsymbol{w}_{1,L}^{(\hat{\mathsf{H}})}$ alone. Receiver two computes a linear combination with nonzero coefficients of $\boldsymbol{w}_{2,L-1}^{(\hat{\mathsf{H}})}$ and $\boldsymbol{w}_{1,L}^{(\hat{\mathsf{H}})}$. Knowing $\boldsymbol{w}_{1,L}^{(\hat{\mathsf{H}})}$, we can thus recover $\boldsymbol{w}_{2,L-1}^{(\hat{\mathsf{H}})}$. Continuing in the same manner, alternating between the receivers in each step, we can successively recover all transmitted messages. This shows that the mapping between the messages at the transmitters and the decoded functions at the receivers is invertible.

Fix a quantized channel realization $\hat{\mathbf{H}}$. Applying L times[3] Lemma 5 in Appendix A guarantees that over the subchannel (38), a computation sum rate (normalized by the number $T^{(\hat{\mathbf{H}})}$ of time slots in the subchannel) arbitrarily close to

$$(2L-1)\log\big(\mathsf{SINR}(\hat{\mathbf{H}})\big)$$

is achievable with average probability of error at most $\varepsilon_2^{(\hat{\mathbf{H}})}(T^{(\hat{\mathbf{H}})}) \to 0$ as $T^{(\hat{\mathbf{H}})} \to \infty$. In terms of the original blocklength T, this translates to a computation sum rate of

$$(2L-1)\frac{T^{(\hat{\mathbf{H}})}}{T}\log\big(\mathsf{SINR}(\hat{\mathbf{H}})\big).$$

Moreover, since $T^{(\hat{\mathbf{H}})} \to \infty$ as $T \to \infty$, and since, for fixed quantization parameter ν there are only finitely many values of $\hat{\mathbf{H}}$, we also have

$$\varepsilon_2(T) \triangleq \max_{\hat{\mathbf{H}}} \varepsilon_2^{(\hat{\mathbf{H}})}(T^{(\hat{\mathbf{H}})}) \to 0$$

as $T \to \infty$.

We repeat the coding procedure above for all quantized channel realizations $\hat{\mathbf{H}}$ with finite magnitudes, i.e., satisfying $\|\hat{\mathbf{H}}\|_\infty < \infty$. The overall computation sum rate is at least

$$\begin{aligned}
&(2L-1)\sum_{\hat{\mathbf{H}}:\|\hat{\mathbf{H}}\|_\infty<\infty}\frac{T^{(\hat{\mathbf{H}})}}{T}\log\big(\mathsf{SINR}(\hat{\mathbf{H}})\big)\\
&\overset{(a)}{\geq}\frac{2L-1}{L}(1-\eta(T))\sum_{\hat{\mathbf{H}}:\|\hat{\mathbf{H}}\|_\infty<\infty}p_{\hat{\boldsymbol{H}}}(\hat{\mathbf{H}})\log\big(\mathsf{SINR}(\hat{\mathbf{H}})\big)\\
&\overset{(b)}{\geq}\frac{2L-1}{L}(1-\eta(T))\sum_{\hat{\mathbf{H}}:\|\hat{\mathbf{H}}\|_\infty<\infty}p_{\hat{\boldsymbol{H}}}(\hat{\mathbf{H}})\bigg(\log\Big(\frac{P/16}{1+2L^2(\pi+1)^2P/\nu^2}\Big)-6\log(c(\hat{\mathbf{H}}))\bigg)\\
&\overset{(c)}{\geq}\frac{2L-1}{L}(1-\eta(T))\bigg((1-\delta(\nu))\log\Big(\frac{P/16}{1+2L^2(\pi+1)^2P/\nu^2}\Big)-6\mathbb{E}\big(\log(c(\hat{\mathbf{H}}));\|\hat{\mathbf{H}}\|_\infty<\infty\big)\bigg),
\end{aligned}$$

where (a) follows from (37), (b) follows from (39), and (c) follows from (4). Here, the $(1-\eta(T))$ factor accounts for the loss in matching the channel gains at times $t_1,\dots,t_L$, and the factor $(1-\delta(\nu))$ accounts for channel realizations that are quantized to ∞, see Section V-A. Both $\eta(T) \to 0$ as the blocklength $T \to \infty$ by (10) and $\delta(\nu) \to 0$ as the quantization parameter $\nu \to \infty$ by (11).

There are two sources of error in this communication scheme: atypicality of the channel gains and atypicality of the noise terms. The channel gains are handled by the matching construction described in Section V-A. We declare an error whenever the channel gains are atypical, which happens with probability at most $\varepsilon_1(T)$ with $\varepsilon_1(T) \to 0$ as $T \to \infty$ for fixed L and ν by (8) and (9). The noise is handled by the computation code over the integer channel. As we have seen above, an error occurs with probability at most $\varepsilon_2(T)$ with $\varepsilon_2(T) \to 0$ as $T \to \infty$ for fixed L and ν. Since the number of finite quantized channel gains is at most $\nu^4 L$ by (2), and since the number of receivers is $2L-1 \leq 2L$ for each such realization of the quantized channel, with probability at least

$$1-\varepsilon_1(T)-2\nu^4L^2\varepsilon_2(T)$$

all decoders are successful. For a fixed number of subblocks L and fixed quantization parameter ν, this quantity converges to one as $T \to \infty$, yielding an achievable computation sum rate of

$$R(P,L,\nu) \triangleq \frac{2L-1}{L}\bigg((1-\delta(\nu))\log\Big(\frac{P/16}{1+2L^2(\pi+1)^2P/\nu}\Big)-6\mathbb{E}\big(\log(c(\hat{\boldsymbol{H}}));\|\hat{\boldsymbol{H}}\|_\infty<\infty\big)\bigg).$$

---

[3] Since the input symbols at the two receivers for different values of $j \in \{1,\dots,L\}$ are coupled, we need to make use of the universality of the channel encoders mentioned after the statement of Lemma 5.

Hence the computation capacity $C(P)$ is lower bounded as

$$C(P) \geq R(P, L, \nu).$$

Since this is true for all values of ν, we may take the limit as $\nu \to \infty$ to obtain

$$\begin{aligned} C(P) &\geq \lim_{\nu \to \infty} R(P, L, \nu) \\ &= \frac{2L-1}{L}\Big(\log(P/16) - 6 \lim_{\nu\to\infty} \mathbb{E}\big(\log(c(\hat{\boldsymbol{H}})); \|\hat{\boldsymbol{H}}\|_\infty < \infty\big)\Big). \end{aligned}$$

In Appendix B, we show that

$$\lim_{\nu\to\infty} \mathbb{E}\big(\log(c(\hat{\boldsymbol{H}})); \|\hat{\boldsymbol{H}}\|_\infty < \infty\big) \leq 3.$$

Thus, the computation capacity is lower bounded by

$$\begin{aligned} C(P) &\geq \lim_{\nu \to \infty} R(P, L, \nu) \\ &= \frac{2L-1}{L}\big(\log(P/16) - 18\big). \end{aligned}$$

Finally, we may take a limit as $L \to \infty$, yielding a computation rate of

$$\begin{aligned} C(P) &\geq \lim_{L\to\infty} \lim_{\nu \to \infty} R(P, L, \nu) \\ &= 2\log(P) - 44 \\ &\geq K \log(P) - 7K^3, \end{aligned}$$

concluding the proof of the lower bound in Theorem 1 for $K = 2$. ■

VI. PROOF OF LOWER BOUND IN THEOREM 1 FOR $K > 2$ USERS

As in the two-user case in Section V, the proof for $K > 2$ proceeds in three steps: matching of channel gains (see Section VI-A), linear precoding and matched filtering (see Section VI-B), and computation of functions of the messages over the resulting channel from the precoder input to the matched filter output (see Section VI-C). We again quantize all channel gains as described in Section IV and consider large blocklengths T such that this quantization can be performed for arbitrarily large quantization parameter ν and such that the resulting observed sequence of quantized channel gains is η-typical with high probability. Since the effects of quantization and atypicality are essentially identical to the two-user case, we will not repeat this analysis here and instead assume directly that $\nu \approx \infty$, which implies that $\hat{h}_{m,k}[t] \approx h_{m,k}[t]$. The quantization and typicality arguments for $K = 2$ carry over for $K > 2$.

A. *Matching of Channel Gains*

Fix a large blocklength T and a natural number I. Define

$$L \triangleq (I+1)^{K^2},$$

and divide the block of T channel realizations into L subblocks of length T/L (assumed to be integer). Consider the channel gains at time $t_1 = 1$ in the first of these blocks and the corresponding channel gains $\boldsymbol{H}[t_1]$. Let t_ℓ be the first time in block ℓ such that[4]

$$h_{m,k}[t_\ell] = \omega_L^{(\ell-1)d_{m,k}} h_{m,k}[t_1]$$

---

[4] The probability of this event happening is, of course, zero. The statement is to be understood in terms of the quantized channel gains $\hat{h}_{m,k}[t]$ and sufficiently large ν so that $\hat{h}_{m,k}[t] \approx h_{m,k}[t]$.

for all $k, m \in \{1, \dots, K\}$, where ω_L is the Lth root of unity as before, and where

$$d_{m,k} \triangleq (I+1)^{(k-1)K+m-1}.$$

Repeat this construction with $t_1 = 2$ and so on, ensuring that no time slot is matched more than once.

By the assumptions of circular symmetry and ergodicity of the fading gains, essentially all but a fraction $o(1)$ of the channel gains can be matched up in this fashion as $T \to \infty$ (see Lemmas 3 and 4), and we will assume in the following that T is large enough to ignore the $o(1)$ term (see Section V-A for a detailed analysis).

B. *Precoding and Matched Filtering*

Consider now one such sequence of matched time slots $t_1, \dots, t_L$. As in the two-user case, we use linear precoders and matched filters over the vector channel induced by these L time slots. Define the diagonal matrix

$$\boldsymbol{D}_{m,k} \triangleq \operatorname{diag}\big((h_{m,k}[t_\ell])_{\ell=1}^{L}\big)$$

corresponding to the vector channel of length L between transmitter k and receiver m at time slots $t_1, \dots, t_L$. By construction,

$$\boldsymbol{D}_{m,k} = h_{m,k}\boldsymbol{F}^{d_{m,k}},$$

where

$$h_{m,k} \triangleq h_{m,k}[t_1]$$

and

$$\boldsymbol{F} \triangleq \operatorname{diag}\big((\omega_L^{\ell-1})_{\ell=1}^{L}\big).$$

Each transmitter uses again a linear precoder with transmit vectors $\boldsymbol{v} \in \mathcal{V} \subset \mathbb{C}^L$. The set $\mathcal{V}$ is constructed as

$$\mathcal{V} \triangleq \bigg\{\boldsymbol{v} = \bigg(\prod_{m,k}\Big(\prod_{\alpha=1}^{\alpha_{m,k}} b_{m,k}^{(\alpha)}\Big)\boldsymbol{D}_{m,k}^{\alpha_{m,k}}\bigg)\boldsymbol{1} : \alpha_{m,k} \in \{0, \dots, I-1\}\bigg\}.$$

Since all channel matrices $\boldsymbol{D}_{m,k}$ are diagonal by construction, the product $\boldsymbol{D}_{m,k}\boldsymbol{D}_{\tilde{m},\tilde{k}}$ commutes, and hence it is immaterial in which order the product in the definition of $\mathcal{V}$ is taken. The scalars $b_{m,k}^{(\alpha)}$ are constructed recursively, starting from $b_{m,k}^{(1)}$. Each $b_{m,k}^{(\alpha)}$ is of the form n or $1/n$ for the smallest natural number $n \in \mathbb{N}$ such that

$$\Big(\prod_{\alpha=1}^{\alpha_{m,k}} b_{m,k}^{(\alpha)}\Big)|h_{m,k}|^{\alpha_{m,k}} \in [1, 2).$$

As in the two-user case, the role of the $b_{m,k}^{(\alpha)}$ is to ensure that the transmit vectors all have approximately the same norm. In particular,

$$\sqrt{L} \leq \|\boldsymbol{v}\| \leq 2^{K^2}\sqrt{L} \tag{40}$$

for every $\boldsymbol{v} \in \mathcal{V}$. Moreover, by the recursive construction,

$$\big(2\max\big\{|h_{m,k}|, |h_{m,k}|^{-1}\big\}\big)^{-1} \leq \min\big\{b_{m,k}^{(\alpha)}, 1/b_{m,k}^{(\alpha)}\big\} \leq \max\big\{b_{m,k}^{(\alpha)}, 1/b_{m,k}^{(\alpha)}\big\} \leq 2\max\big\{|h_{m,k}|, |h_{m,k}|^{-1}\big\}, \tag{41}$$

and hence

$$\big(2^{K^2}c\big)^{-1} \leq \prod_{m,k}\min\big\{b_{m,k}^{(\alpha_{m,k})}, 1/b_{m,k}^{(\alpha_{m,k})}\big\} \leq \prod_{m,k}\max\big\{b_{m,k}^{(\alpha_{m,k})}, 1/b_{m,k}^{(\alpha_{m,k})}\big\} \leq 2^{K^2}c \tag{42}$$

for all $\alpha_{m,k} \in \{0, \dots, I-1\}$, and where

$$c = c(\boldsymbol{H}) \triangleq \prod_{m,k} \max\big\{|h_{m,k}|, |h_{m,k}|^{-1}\big\}. \tag{43}$$

Observe that, as in the two-user case, each transmit vector $\boldsymbol{v} \in \mathcal{V}$ is of the form

$$\boldsymbol{v} = \rho \boldsymbol{F}^{\alpha}\mathbf{1}$$

for some scalars $\rho \in \mathbb{C}$ and $\alpha \in \mathbb{N}$. By (16), this implies that any two transmit vectors in $\mathcal{V}$ are either collinear or orthogonal. As we will see next, all vectors in $\mathcal{V}$ are, in fact, orthogonal.

Each $\boldsymbol{v} \in \mathcal{V}$ is a complex-valued vector of length L defined by a monomial up to power $I-1$ in the channel matrices $\boldsymbol{D}_{m,k}$. By definition, every collection of powers $\alpha_{m,k} \in \{0, \dots, I-1\}, m, k \in \{1, \dots, K\}$ corresponds to an element $\boldsymbol{v} \in \mathcal{V}$. We now argue that this correspondence is one-to-one. implying that

$$|\mathcal{V}| = I^{K^2},$$

Moreover, together with the argument in the last paragraph, this will also ensure that all vectors in $\mathcal{V}$ are orthogonal.

To this end, consider $\boldsymbol{v} \in \mathcal{V}$ and write it as

$$\boldsymbol{v} = \rho\Big(\prod_{m,k} \boldsymbol{F}^{d_{m,k}\alpha_{m,k}}\Big)\mathbf{1}$$

for some $\alpha_{m,k} \in \{0, \dots, I-1\}$ and scalar ρ. The first component of $\boldsymbol{v}$ is equal to ρ. The second component of $\boldsymbol{v}$ is equal to $\rho\omega_L^{\alpha}$ with

$$\begin{aligned}\alpha &\triangleq \sum_{m,k} \alpha_{m,k} d_{m,k} \pmod L \\ &= \sum_{m,k} \alpha_{m,k}(I+1)^{(k-1)K+m-1} \pmod L.\end{aligned}$$

Since each $\alpha_{m,k} \in \{0, \dots, I-1\}$, this last sum is less than L, and so the modulo L operation can be dropped. Thus, the coefficients $\alpha_{m,k}$ of α can be determined uniquely by computing the $(I+1)$-ary expansion of α. Moreover, knowing ρ from the first component of $\boldsymbol{v}$, α can be uniquely determined from the second component of $\boldsymbol{v}$. Together, this shows that there is a unique collection of powers $\alpha_{m,k} \in \{0, \dots, I-1\}$ for all $m, k \in \{1, \dots, K\}$ that generates $\boldsymbol{v}$. We refer to this as the *unique factorization* property of $\mathcal{V}$. Since each exponent α corresponds to a unique $\boldsymbol{v} \in \mathcal{V}$, this also shows the orthogonality of the vectors in $\mathcal{V}$.

Each transmitter modulates I^{K^2} zero mean and mutually independent message symbols over its transmit vectors. Let $s_{k,\boldsymbol{v}}$ be the message symbol at transmitter k sent along transmit vector $\boldsymbol{v} \in \mathcal{V}$. The channel input

$$\boldsymbol{x}_k \triangleq \begin{pmatrix} x_k[t_1] & x_k[t_2] & \cdots & x_k[t_L]\end{pmatrix}^{\mathsf{T}}$$

at transmitter k has then the form

$$\boldsymbol{x}_k = \sum_{\boldsymbol{v} \in \mathcal{V}} s_{k,\boldsymbol{v}}\boldsymbol{v}.$$

We allocate the same power

$$\mathbb{E}\big(|s_{k,\boldsymbol{v}}|^2\big) = \frac{P}{4^{K^2}L} \triangleq \tilde{P} \tag{44}$$

to each $s_{k,\boldsymbol{v}}$. Since each transmit vector $\boldsymbol{v}$ has squared norm at most $4^{K^2}L$ by (40), we have

$$\frac{1}{L}\mathbb{E}\big(\|\boldsymbol{x}_k\|^2\big) \le \frac{|\mathcal{V}|}{L} \times \frac{P}{4^{K^2}L} \times 4^{K^2}L \le P,$$

satisfying the average power constraint over the L time slots $t_1, \dots, t_L$. Since each of the K transmitters has I^{K^2} transmit vectors, we transmit a total of KI^{K^2} independent data streams over $L = (I+1)^{K^2}$ channel uses.

The corresponding vector of channel outputs

$$\boldsymbol{y}_m \triangleq \begin{pmatrix} y_m[t_1] & y_m[t_2] & \cdots & y_m[t_L] \end{pmatrix}^{\mathsf{T}}$$

at receiver m is then

$$\begin{aligned} \boldsymbol{y}_m &= \sum_{k=1}^{K} \boldsymbol{D}_{m,k} \boldsymbol{x}_k + \boldsymbol{z}_m \\ &= \sum_{k=1}^{K} \sum_{\boldsymbol{v} \in \mathcal{V}} s_{k,\boldsymbol{v}} \boldsymbol{D}_{m,k} \boldsymbol{v} + \boldsymbol{z}_m, \end{aligned} \tag{45}$$

where

$$\boldsymbol{z}_m \triangleq \begin{pmatrix} z_m[t_1] & z_m[t_2] & \cdots & z_m[t_L] \end{pmatrix}^{\mathsf{T}}$$

is the additive noise at receiver m.

From (45), transmit vector $\boldsymbol{v} \in \mathcal{V}$ is observed at receiver m as $\boldsymbol{D}_{m,k}\boldsymbol{v}$. Each receiver m the receive vectors

$$\tilde{\mathcal{V}}_m \triangleq \big\{ \tilde{\boldsymbol{v}} = \boldsymbol{D}_{m,k}\boldsymbol{v} / \|\boldsymbol{D}_{m,k}\boldsymbol{v}\| : k \in \{1, \dots, K\}, \boldsymbol{v} \in \mathcal{V} \big\} \subset \mathbb{C}^L$$

as matched filters, computing $\tilde{\boldsymbol{v}}^\dagger \boldsymbol{y}_m$ for each $\tilde{\boldsymbol{v}} \in \tilde{\mathcal{V}}_m$. The number of matched filters is at most

$$|\tilde{\mathcal{V}}_m| \leq (I+1)^{K^2}.$$

By the same argument as for $\mathcal{V}$, it can be shown that $\tilde{\mathcal{V}}_m$ also has the unique factorization property. In other words, to every $\tilde{\boldsymbol{v}} \in \tilde{\mathcal{V}}_m$ corresponds a unique collection of powers $\alpha_{m,k} \in \{0, \dots, I\}$ for all $m, k \in \{1, \dots, K\}$ such that

$$\tilde{\boldsymbol{v}} = \frac{1}{\sqrt{L}} \Big(\prod_{m,k} \boldsymbol{F}^{\alpha_{m,k} d_{m,k}} \Big) \boldsymbol{1}.$$

As for $\mathcal{V}$, this implies that the vectors in $\tilde{\mathcal{V}}_m$ are orthogonal by the properties of the "Fourier" matrix $\boldsymbol{F}$.

The equivalent channel, consisting of the linear precoder, the wireless channel, and the matched filters, has I^{K^2} channel inputs at each transmitter and at most $(I+1)^{K^2}$ channel outputs at each receiver. Since the matched filters are normalized to have unit norm, each such subchannel at the receiver is an additive Gaussian noise channel with unit noise power. We now argue that we have again signal alignment as in the two-user case.

As pointed out above, the transmit vector $\boldsymbol{v} \in \mathcal{V}$ at transmitter k is observed at receiver m as $\boldsymbol{D}_{m,k}\boldsymbol{v}$. By construction of the set of matched filter vectors $\tilde{\mathcal{V}}_m$ at receiver m, $\boldsymbol{D}_{m,k}\boldsymbol{v}$ is a scalar multiple of a vector $\tilde{\boldsymbol{v}} \in \tilde{\mathcal{V}}_m$. Since all the vectors in $\tilde{\mathcal{V}}_m$ are orthogonal, this implies that the matched filtering operation $\tilde{\boldsymbol{v}}^\dagger \boldsymbol{y}_m$ removes all but those transmit signals which are aligned with $\tilde{\boldsymbol{v}}$.

We now analyze the magnitudes of the signals that are observed along one receive vector $\tilde{\boldsymbol{v}} \in \tilde{\mathcal{V}}_m$ at receiver m. By unique factorization, there exists a unique collection of exponents $\alpha_{\tilde{m},\tilde{k}} \in \{0, \dots, I\}$ such that

$$\tilde{\boldsymbol{v}} = \rho \Big(\prod_{\tilde{m},\tilde{k}} \boldsymbol{D}_{\tilde{m},\tilde{k}}^{\alpha_{\tilde{m},\tilde{k}}} \Big) \boldsymbol{1}$$

for some scalar ρ. Assume a signal modulated over transmit vector $\boldsymbol{v}_k$ at transmitter k is observed along vector $\tilde{\boldsymbol{v}}$ at receiver m. Note that this is only possible if $\alpha_{m,k} \in \{1, \dots, I\}$ and $\alpha_{\tilde{m},\tilde{k}} \in \{0, \dots, I-1\}$ for all $(\tilde{m}, \tilde{k}) \neq (m,k)$. The transmit vector $\boldsymbol{v}_k$ has then to be equal to

$$\boldsymbol{v}_k = \Big(\prod_{\alpha=1}^{\alpha_{m,k}-1} b_{m,k}^{(\alpha)} \Big) \boldsymbol{D}_{m,k}^{\alpha_{m,k}-1} \Big(\prod_{(\tilde{m},\tilde{k}) \neq (m,k)} \Big(\prod_{\alpha=1}^{\alpha_{\tilde{m},\tilde{k}}} b_{\tilde{m},\tilde{k}}^{(\alpha)} \Big) \boldsymbol{D}_{\tilde{m},\tilde{k}}^{\alpha_{\tilde{m},\tilde{k}}} \Big) \boldsymbol{1}.$$

Defining

$$b \triangleq \frac{\prod_{\tilde{m},\tilde{k}} \prod_{\alpha=1}^{\alpha_{\tilde{m},\tilde{k}}} b_{\tilde{m},\tilde{k}}^{(\alpha)}}{\prod_{\tilde{k}} b_{m,\tilde{k}}^{(\alpha_{m,\tilde{k}})}},$$

and

$$b_k \triangleq \prod_{\tilde{k} \neq k} b_{m,\tilde{k}}^{(\alpha_{m,\tilde{k}})}, \tag{46}$$

this allows to write $\boldsymbol{v}_k$ in terms of $\tilde{\boldsymbol{v}}$ as

$$\boldsymbol{v}_k = \frac{b}{\rho} b_k \boldsymbol{D}_{m,k}^{-1} \tilde{\boldsymbol{v}} \in \mathcal{V}. \tag{47}$$

Since the collection of exponents $\alpha_{\tilde{m},\tilde{k}}$ corresponding to $\tilde{\boldsymbol{v}}$ is unique, and by orthogonality of $\mathcal{V}$, this implies that there are at most K signals that are aligned along the same vector $\tilde{\boldsymbol{v}}$ at receiver m, and they are all observed with the same common channel gain times a factor b_k depending on the transmitter k. Using the orthogonality of the matched filters and (47), the output of the matched filter applied to the channel output (45) can then be written as

$$\begin{aligned}
\tilde{\boldsymbol{v}}^\dagger \boldsymbol{y}_m &= \sum_{k=1}^{K} \sum_{\boldsymbol{v} \in \mathcal{V}} s_{k,\boldsymbol{v}} \tilde{\boldsymbol{v}}^\dagger \boldsymbol{D}_{m,k} \boldsymbol{v} + \tilde{\boldsymbol{v}}^\dagger \boldsymbol{z}_m \\
&= \sum_{k=1}^{K} s_{k,\boldsymbol{v}_k} \tilde{\boldsymbol{v}}^\dagger \boldsymbol{D}_{m,k} \boldsymbol{v}_k + \tilde{z}_{m,\tilde{\boldsymbol{v}}} \\
&= \frac{b}{\rho} \sum_{k=1}^{K} b_k s_{k,\boldsymbol{v}_k} + \tilde{z}_{m,\tilde{\boldsymbol{v}}},
\end{aligned} \tag{48}$$

where

$$\tilde{z}_{m,\tilde{\boldsymbol{v}}} \triangleq \tilde{\boldsymbol{v}}^\dagger \boldsymbol{z}_m$$

is additive circularly-symmetric complex Gaussian noise with mean zero and variance one, and where $\boldsymbol{v}_k = \boldsymbol{v}_k(\tilde{\boldsymbol{v}}, m)$ depends on both the matched filter $\tilde{\boldsymbol{v}}$ and the receiver m. We can interpret (48) as a subchannel between the inputs to the precoder $\boldsymbol{v}_k$ at each transmitter k and the output of matched filter $\tilde{\boldsymbol{v}}$ at receiver m.

We point out that, similar to the two-user case, not all K transmitters contribute to all matched filter outputs $\tilde{\boldsymbol{v}}^\dagger \boldsymbol{y}_m$. Indeed, if $\alpha_{m,k} = 0$ in the unique factorization of $\tilde{\boldsymbol{v}}$ at receiver m, then there is no corresponding transmit vector $\boldsymbol{v}_k$ at transmitter k. For ease of notation, we assume that $s_{k,\boldsymbol{v}_k} = 0$ in this case, so that (48) is still valid.

We now bound the channel gains in the matched filter output (48). From (47), we have

$$|b/\rho| = \frac{\|\boldsymbol{v}_k\|}{b_k \|\boldsymbol{D}_{m,k}^{-1} \tilde{\boldsymbol{v}}\|} = \frac{|h_{m,k}| \|\boldsymbol{v}_k\|}{b_k}.$$

By (41), (43), and (46),

$$|h_{m,k}|^{-1} b_k = |h_{m,k}|^{-1} \prod_{\tilde{k} \neq k} b_{m,\tilde{k}}^{(\alpha_{m,\tilde{k}})} \leq 2^K c.$$

Together with (40), this shows that

$$|b/\rho| \geq \frac{\sqrt{L}}{2^K c} \tag{49}$$

Moreover, each b_k is is a product of at most K scalars, each being either a natural number or its inverse.

We want to multiply the output of the subchannel (48) by a positive scalar $\tilde{\rho}$ such that $\tilde{\rho} b_k \in \mathbb{N}$ for all k. By the definition of b_k in (46), we can choose

$$\tilde{\rho} \triangleq \prod_{\tilde{k}=1}^{K} \max\big\{1, 1/b_{m,\tilde{k}}^{(\alpha_{m,\tilde{k}})}\big\}.$$

Using (41) and (42), we thus have

$$\tilde{\rho} \leq 2^K c, \tag{50}$$

resulting in a decrease of effective signal power by at most a factor $4^K c^2$.

To summarize, the channel (48) between the input $s_{k,\boldsymbol{v}_k}$ to the matched filter at transmitter k and the output of the matched filter $\tilde{\boldsymbol{v}} \in \tilde{\mathcal{V}}$ at receiver m is of the form

$$r_{m,\tilde{\boldsymbol{v}}} = \beta_{m,\tilde{\boldsymbol{v}}} \sum_{k=1}^{K} a_k s_{k,\boldsymbol{v}_k} + \mu_{m,\tilde{\boldsymbol{v}}}, \tag{51}$$

for nonzero integer channel gains a_k, scaled Gaussian noise $\mu_{m,\tilde{\boldsymbol{v}}}$, and positive scaling factor $\beta_{m,\tilde{v}}$. Using (44), (49), and (50), the signal-to-interference-and-noise ratio SINR of this subchannel is lower bounded by

$$\begin{aligned} \mathsf{SINR} &\geq \frac{\tilde{P}|b/\rho|^2}{\tilde{\rho}^2} \\ &\geq \frac{P/(4^{K^2}L) \times L/(4^K c^2)}{4^K c^2} \\ &\geq \frac{P}{2^{4K+2K^2} c^4}. \end{aligned} \tag{52}$$

C. Computation of Functions

We use a computation code over the channel from the precoder input to the matched filter output constructed in the last section. This will allow us to reliably decode functions of the transmitted messages over this channel.

As in the proof of the two-user case, we code over several channel uses, each with the same channel realization $\mathbf{H}$. For each such $\mathbf{H}$, we are hence dealing with a channel that is constant across time. Each transmitter k splits its message w_k into non-overlapping submessages, one for each subchannel (51) between precoder input and matched filter output, and for each channel realization $\mathbf{H}$. Each such submessage is again a vector over $\{0, \dots, q-1\}$ for some q. The decoder aims to compute a modulo-q integer linear equation of these messages with coefficients a_k as appearing in (51).

Using the unique factorization property of $\tilde{\mathcal{V}}$ and the fact that all coefficients a_k are nonzero, it follows from [4, Lemma 8] that the functions to be decoded by the receivers can be inverted. Hence, knowledge of all correctly decoded functions at the receivers allows recovery of all the messages.

Applying L times[5] Lemma 5 in Appendix A shows then that each of the receivers can reliably compute its desired functions over the channel given by (51) at a sum rate at least

$$KI^{K^2} \log\big(\mathsf{SINR}(\mathbf{H})\big) \geq \log(P) - 4K - 2K^2 - 4\log(c(\mathbf{H}))$$

for a particular realization $\mathbf{H}$ of the channel gains, and where we have used (52), that the number of transmitted messages is $|\mathcal{V}| = I^{K^2}$, and that there are K receivers. Normalizing by the number $(I+1)^{K^2}$ of channel uses, we can hence achieve a sum rate of at least

$$R(P, I) \triangleq \frac{KI^{K^2}}{(I+1)^{K^2}} \Big(\log(P) - 4K - 2K^2 - 4\mathbb{E}\big(\log(c(\boldsymbol{H}))\big)\Big)$$

---

[5] As in the two-user case, the input symbols at the K receivers are coupled. We make again use of the universality of the channel encoders mentioned after the statement of Lemma 5.

when averaged over all channel realizations.

The computation sum capacity is then lower bounded as

$$C(P) \geq R(P, I).$$

Since this holds for all values of I, and since the constant c does not depend on I, we may take the limit as $I \to \infty$ to obtain a computation rate of at least

$$\begin{aligned} C(P) &\geq \lim_{I \to \infty} R(P, I) \\ &= K \log(P) - 4K^2 - 2K^3 - 4K\mathbb{E}\big(\log(c(\boldsymbol{H}))\big) \\ &\geq K \log(P) - 7K^3, \end{aligned}$$

where we have used the upper bound on the expected value of $\log(c(\boldsymbol{H}))$ in Appendix B. This concludes the proof of the lower bound in Theorem 1 for arbitrary $K \geq 2$. ■

VII. PROOF OF UPPER BOUND IN THEOREM 1

The proof adapts an argument from [40, Theorem 4].

Since the receivers compute an invertible function of the messages, the cut-set bound [41, Theorem 14.10.1] applies, showing that

$$C(P) \leq \sup_{\boldsymbol{Q}(\boldsymbol{H})} \mathbb{E}\big(\log\det(\boldsymbol{I} + \boldsymbol{H}\boldsymbol{Q}(\boldsymbol{H})\boldsymbol{H}^\dagger)\big),$$

where the maximization is over all positive semidefinite matrices $\boldsymbol{Q}(\boldsymbol{H})$ such that

$$\mathbb{E}\big(\operatorname{tr}(\boldsymbol{Q}(\boldsymbol{H}))\big) \leq KP.$$

Using Hadamard's inequality, this can be upper bounded as

$$\begin{aligned} \sup_{\boldsymbol{Q}(\boldsymbol{H})} \mathbb{E}\big(\log\det(\boldsymbol{I} + \boldsymbol{H}\boldsymbol{Q}(\boldsymbol{H})\boldsymbol{H}^\dagger)\big) &\leq \sum_{m=1}^{K} \sup_{\boldsymbol{Q}(\boldsymbol{H})} \mathbb{E}\big(\log(1 + \boldsymbol{h}_m \boldsymbol{Q}(\boldsymbol{H})\boldsymbol{h}_m^\dagger)\big) \\ &\leq K \sup_{P(r)} \mathbb{E}\big(\log(1 + rP(r))\big), \end{aligned}$$

where $\boldsymbol{h}_m$ denotes the mth row of $\boldsymbol{H}$, where

$$r \triangleq \|\boldsymbol{h}_1\|^2,$$

and where the last maximization is over all nonnegative $P(r)$ satisfying

$$\mathbb{E}(P(r)) \leq KP.$$

This upper bound on $C(P)$ is maximized by water-filling [42], yielding

$$C(P) \leq K\mathbb{E}\big(\log(1 + rP^\star(r))\big)$$

with

$$P^\star(r) \triangleq \Big(\frac{1}{\mu} - \frac{1}{r}\Big)^+$$

and μ such that

$$\mathbb{E}(P^\star(r)) = KP. \tag{53}$$

Since

$$P^\star(r) \leq \frac{1}{\mu},$$

we can further upper bound

$$\begin{aligned} C(P) &\leq K\mathbb{E}(\log(1+r/\mu)) \\ &\leq K\log(1+\mathbb{E}(r)/\mu), \end{aligned} \tag{54}$$

where we have used Jensen's inequality.

It remains to lower bound μ. By (53), we have

$$\begin{aligned} KP &= \mathbb{E}(P^\star(r)) \\ &= \int_{\mathsf{r}=\mu}^{\infty} \Big(\frac{1}{\mu} - \frac{1}{\mathsf{r}}\Big) f_r(\mathsf{r}) d\mathsf{r} \\ &\geq \int_{\mathsf{r}=2\mu}^{\infty} \Big(\frac{1}{\mu} - \frac{1}{\mathsf{r}}\Big) f_r(\mathsf{r}) d\mathsf{r} \\ &\geq \frac{1}{2\mu}\mathbb{P}(r \geq 2\mu). \end{aligned}$$

The random variable r has Erlang distribution with parameter K and rate one, and hence

$$\begin{aligned} KP &\geq \frac{1}{2\mu}\mathbb{P}(r \geq 2\mu) \\ &= \frac{1}{2\mu}\sum_{k=0}^{K-1} \exp(-2\mu)\frac{(2\mu)^k}{k!} \\ &\geq \frac{1}{2\mu}\exp(-2\mu). \end{aligned}$$

If $\mu \leq 1/4KP$, then we obtain the contradiction

$$\begin{aligned} KP &\geq \frac{1}{2\mu}\exp(-2\mu) \\ &\geq 2KP\exp(-1/2KP) \\ &> KP \end{aligned}$$

for $K \geq 2$, $P \geq 1$. Hence $\mu > 1/4KP$.

Substituting this into (54) yields

$$\begin{aligned} C(P) &\leq K\log(1+4KP\mathbb{E}(r)) \\ &= K\log(1+4K^2P) \\ &\leq K\log(P) + 5K\log(K), \end{aligned}$$

where we have used $P \geq 1$ and $K \geq 2$. This concludes the proof of the upper bound in Theorem 1. ■

VIII. PROOF OF THEOREM 2

This section provides the proof for the approximation result of the sum capacity $C^{(D)}(P)$ of the D-layer relay network. The proof builds on the approximation result for the computation sum rate in Theorem 1. Since the upper bound in Theorem 2 follows directly from the same cut-set bound argument as Theorem 1, we focus here on the lower bound.

Each of the D network layers operates using compute-and-forward. We use the same codebook rate $R_k = R$ at each source node $k \in \{1, \dots, K\}$. Using Theorem 1, the relay nodes at layer one can then reliably decode a deterministic invertible function of the messages at sum rate at least

$$K\log(P) - 7K^3.$$

Since the blocklength used is arbitrarily long, the probability of decoding error at the relays can be made smaller than ε/D for any $\varepsilon > 0$.

The relays in layer one treat these computed functions as their messages for the destination node, and re-encode them using again a computation code. In order to make this argument inductively, we will apply Theorem 1 for each layer. Two difficulties arise. First, the statement in Theorem 1 is only for the computation *sum rate* and it is not clear how much each individual transmitter and receiver contributes to this sum. For the induction argument, we need to argue that we can choose the message rates at the transmitters to be symmetric, and that we can choose the rates of the decoded functions at the receivers to be symmetric. Second, the definition of computation capacity stipulates only that the receivers decode an invertible deterministic function of the messages. In particular, the sum rate of the decoded functions at any receiver could be larger than the sum rate of the transmitted messages. For example, if a receiver decodes a sum over $\mathbb{Z}$ of two messages, then the entropy of this decoded function is larger than the entropy of either of the messages. For the induction argument, we need to argue that the we can choose the functions to be computed at the receivers to be over the same alphabet as the messages at the transmitters, thus avoiding growth of the messages as they traverse the network.

From the proof of Theorem 1, we see that the rates of the messages at the transmitters as well as the rates of the computed functions at the receivers are indeed symmetric as the time expansion parameter $L \to \infty$ (see Sections V-C and VI-C). Moreover, the messages at the transmitters as well as the computed functions at the receivers are all over the same finite field of size q (see again Sections V-C and VI-C). Thus, the message sizes do not increase as they traverse the network.

We can therefore inductively apply Theorem 1 to conclude that the relays at layer d in the network can decode a deterministic invertible function of the messages at layer $d-1$ for all $d \in \{1, \ldots, D\}$ at sum rate at least

$$K \log(P) - 7K^3.$$

Since the composition of invertible functions is invertible, this implies that the relay nodes in layer D compute a deterministic invertible function of the messages at the source at this sum rate.

Since the relay nodes in the last layer are connected to the destination node by orthogonal bit pipes of infinite capacity, they can forward their computed message to the destination. The destination node, in turn, can then invert these K functions to recover the original messages. Since the probability of decoding error is at most ε/D in each layer, this implies that the destination node decodes in error with probability at most ε by the union bound. Since $\varepsilon > 0$ is arbitrary, this proves the lower bound in Theorem 2. ■

IX. CONCLUSIONS

We have considered time-varying Gaussian relay networks consisting of K source nodes communicating to a destination node with the help of D layers of K relay nodes. We have presented a capacity approximation for this type of communication network. The gap in this approximation depends only on the number of source nodes K and the fading statistics, but is independent of the depth D of the network and the transmit power P. This contrasts with previously known approximation results, which have a gap that increases linearly with the depth D of the network.

At the heart of our achievable scheme is the concept of computation alignment, combining computation codes with signal alignment. The use of computation codes allows the relay nodes to remove receiver noise, thus preventing noise from accumulating as messages traverse the network. The use of signal alignment allows the transformation of the wireless channel with time-varying complex-valued channel gains into subchannels with constant integer-valued channel gains, over which these computation codes can be used efficiently.

APPENDIX A
COMPUTATION OVER INTEGER CHANNELS

The channel matching and precoding / matched filtering steps in Sections V and VI transform the time-varying linear channel with arbitrary complex channel gains into a constant linear channel with integer channel gains. In this section, we analyze how to reliably compute functions over this channel. We will employ the compute-and-forward scheme from [3], being well-suited for such constant linear channels with integer channel gains.

Throughout this section, we consider the subchannels (38) and (51). Specifically, relay m observes

$$r_m[t] \triangleq \beta \sum_{k=1}^{K} a_{m,k} s_k[t] + \mu_m[t] \tag{55}$$

where $\beta > 0$ is a positive real scaling factor, $a_{m,k} \in \mathbb{Z}$ are integer channel coefficients, $s_k[t] \in \mathbb{C}$ are the symbols sent by transmitter k, and

$$\mu_m[t] \triangleq \sum_{k=1}^{K} e_{m,k}[t] s_k[t] + \theta_m[t] + z_m[t] \in \mathbb{C}$$

is the sum of interference and noise terms. Part of the interference is due to residual channel fluctuations $e_{m,k}[t]$ and the remainder is due to leakage from other subchannels written as $\theta_m[t]$. We assume that

$$|e_{m,k}[t]| \leq \gamma^2$$

for all m, k, and for some finite constant γ^2 not depending on m, k, t. Finally, $z_m[t]$ is i.i.d. circularly symmetric Gaussian noise with mean zero and variance one. Each leakage term $\theta_m[t]$ has expected power

$$\mathbb{E}\big(|\theta_m[t]|^2\big) \leq \sigma^2$$

and is independent of the symbols $s_k[t]$ for all $m, k,$ and t. Over a block of length T, we impose an average power constraint of

$$\frac{1}{T} \sum_{t=1}^{T} |s_k[t]|^2 \leq P.$$

It will be convenient to express the messages at the transmitters as well as the functions computed at the receivers in some finite field.[6] To this end, we write the message w_k at transmitter k as a vector $\boldsymbol{w}_k$ of length κ with components in $\{0, \ldots, q-1\}$ for some prime number q. Receiver m aims to recover the function

$$\boldsymbol{u}_m \triangleq \sum_{k=1}^{K} a_{m,k} \boldsymbol{w}_k \pmod{q}$$

where $a_{m,k}$ are the same integer-valued coefficients that appear in (55). We will assume that these coefficients are chosen so that the resulting functions are invertible. Since we transmit K messages with alphabet size q^κ over T channel uses, the computation sum rate (in bits per channel use) is

$$K \frac{\kappa}{T} \log(q).$$

The following theorem, which is a special case of [3, Theorem 1], lower bounds the computation sum capacity of the channel (55).

Lemma 5. *The computation sum capacity of the channel* (55) *is lower bounded by*

$$K \log(\mathsf{SINR})$$

with

$$\mathsf{SINR} \triangleq \frac{\beta^2 P}{1 + \sigma^2 + K\gamma^2 P}.$$

---

[6] This property will be quite useful in the analysis of D-layer relay networks as it ensures that the rates of the recovered functions are the same as the transmitted messages.

We point out that the codebooks at the K transmitters in Lemma 5 are chosen independently of the coefficients $a_{m,k}$. In other words, the encoders are universal with respect to the channel and equation coefficients $a_{m,k}$.

Proof of Lemma 5: We provide an outline of the proof of Lemma 5 and refer interested readers to [3] for a comprehensive treatment.

Since the channel coefficients are integers, the real and imaginary parts of the inputs will not mix. Therefore, we can write the length T complex-valued channel input and output vectors as length $2T$ real-valued vectors, and treat the channel as essentially a real channel of blocklength $2T$.

To ensure that integer combinations of codewords are themselves codewords, each transmitter employs a *nested lattice codebook* [43]. Formally, a lattice $\Lambda \subset \mathbb{R}^{2T}$ is a discrete subgroup of $2T$-dimensional Euclidean space, and has therefore the property that $\boldsymbol{\lambda}_1, \boldsymbol{\lambda}_2 \in \Lambda$ implies $\boldsymbol{\lambda}_1 + \boldsymbol{\lambda}_2 \in \Lambda$. To construct a nested lattice codebook, we first generate two lattices $\Lambda_{\mathsf{F}} \subset \mathbb{R}^{2T}$ and $\Lambda_{\mathsf{C}} \subset \mathbb{R}^{2T}$ such that $\Lambda_{\mathsf{C}} \subset \Lambda_{\mathsf{F}} \subset \mathbb{R}^{2T}$, i.e., Λ_{C} is a sublattice of Λ_{F}. We refer to Λ_{C} as the *coarse lattice* and to Λ_{F} as the *fine lattice*. The codewords are those elements of the fine lattice Λ_{F} that fall into the fundamental Voronoi region $\mathcal{V}$ of the coarse lattice Λ_{C}.

All transmitters use the same $2T$-dimensional nested lattice code. Each message vector $\boldsymbol{w}_k$ is mapped into a lattice point $\boldsymbol{\lambda}_k \in \Lambda_{\mathsf{F}} \cap \mathcal{V}$. This mapping is one-to-one, i.e., to each $\boldsymbol{\lambda}_k \in \Lambda_{\mathsf{F}} \cap \mathcal{V}$ corresponds a unique message vector $\boldsymbol{w}_k$. Moreover, this mapping can be chosen to preserve linearity (see [3, Lemma 5, Lemma 6]).

To each encoded lattice point we add a random dither $\boldsymbol{d}_k$ generated independently and uniformly over $\mathcal{V}$ to get the length $2T$ channel input

$$\boldsymbol{s}_k \triangleq \boldsymbol{\lambda}_k + \boldsymbol{d}_k \pmod{\Lambda_{\mathsf{C}}}$$

where $\pmod{\Lambda_{\mathsf{C}}}$ denotes ordinary addition in $\mathbb{R}^{2T}$ modulo the coarse lattice Λ_{C}. By [43, Lemma 1], due to the random dither, the signal $\boldsymbol{s}_k$ is independent of the lattice point $\boldsymbol{\lambda}_k$. We make all of the dither vectors available to all relays as common randomness.

The (scaled) channel output can be written as

$$\beta^{-1}\boldsymbol{r}_m = \sum_{k=1}^{K} a_{m,k}\boldsymbol{s}_k + \beta^{-1}\boldsymbol{\mu}_m.$$

Since all receivers are assumed to have access to the dithers, receiver m can remove them from its desired integer combination to form

$$\beta^{-1}\boldsymbol{r}_m - \sum_{k=1}^{K} a_{m,k}\boldsymbol{d}_k = \sum_{k=1}^{K} a_{m,k}\boldsymbol{\lambda}_k + \beta^{-1}\boldsymbol{\mu}_m \pmod{\Lambda_{\mathsf{C}}}.$$

Due to the dithering step, the vector $\boldsymbol{\mu}_m$ is the sum of terms that are all independent of the lattice points $\boldsymbol{\lambda}_k$. Hence, $\boldsymbol{\mu}_m$ can be treated as additive noise. Its expected power is upper bounded by

$$\frac{1}{2T}\mathbb{E}\big(\|\boldsymbol{\mu}_m\|^2\big) \leq 1 + \sigma^2 + K\gamma^2 P.$$

Following the arguments in [3, Theorem 1], all K relays can recover the lattice point

$$\sum_{k=1}^{K} a_{m,k}\boldsymbol{\lambda}_k \pmod{\Lambda_{\mathsf{C}}},$$

and hence decode their equations

$$\sum_{k=1}^{K} a_{m,k}\boldsymbol{w}_k \pmod{q},$$

with vanishing probability of error if the rate if the lattice codebook satisfies

$$\frac{1}{2T}\log\left|\Lambda_{\mathsf{F}}\cap\mathcal{V}\right| < \frac{1}{2}\log\Big(\frac{\beta^2 P}{1+\sigma^2+K\gamma^2 P}\Big).$$

Since there are K receivers, and since one channel use of the original complex channel corresponds to two channel uses of the real channel, the computation sum rate is

$$K\log\Big(\frac{\beta^2 P}{1+\sigma^2+K\gamma^2 P}\Big).$$

Finally, since this scheme works with expectation over the random dithers, there is (at least) one set of fixed dithers that can attain this performance, and therefore no common randomness is actually necessary. ■

APPENDIX B
UPPER BOUND ON THE EXPECTED VALUE OF $\log(c(\hat{\boldsymbol{H}}))$

In this section, we derive the upper bound

$$\lim_{\nu\to\infty}\mathbb{E}\big(\log(c(\hat{\boldsymbol{H}}));\|\hat{\boldsymbol{H}}\|_\infty<\infty\big)\leq\frac{3K^2}{4}$$

as the quantization parameter $\nu\to\infty$.

The term c depends on the quantized channel gains $\hat{\boldsymbol{H}}$, and hence, implicitly, on the channel gains $\boldsymbol{H}$ and the quantization parameter ν. With slight abuse of notation, we write

$$c(\hat{\boldsymbol{H}})=c(\boldsymbol{H},\nu).$$

We then have

$$\begin{aligned}\mathbb{E}\big(\log(c(\hat{\boldsymbol{H}}));\|\hat{\boldsymbol{H}}\|_\infty<\infty\big) &= \sum_{\hat{\mathsf{H}}:\|\hat{\mathsf{H}}\|_\infty<\infty}\log(c(\hat{\boldsymbol{H}}))p_{\hat{\boldsymbol{H}}}(\hat{\mathsf{H}})\\ &= \sum_{\hat{\mathsf{H}}:\|\hat{\mathsf{H}}\|_\infty<\infty}\log(c(\hat{\boldsymbol{H}}))\int_{\mathsf{H}\in Q^{-1}(\hat{\mathsf{H}})}f_{\boldsymbol{H}}(\mathsf{H})d\mathsf{H}\\ &= \int_{\mathsf{H}:\|\mathsf{H}\|_\infty\leq\nu}\log(c(\mathsf{H},\nu))f_{\boldsymbol{H}}(\mathsf{H})d\mathsf{H}\\ &= \mathbb{E}\big(\log(c(\boldsymbol{H},\nu));\|\boldsymbol{H}\|_\infty\leq\nu\big)\end{aligned}$$

by Fubini's theorem, and where $f_{\boldsymbol{H}}$ denotes the density of $\boldsymbol{H}$ and Q the operation of the quantizer.

From the definition of c, and using (5),

$$\begin{aligned}c(\boldsymbol{H},\nu) &= \prod_{m,k}\max\big\{|\hat{h}_{m,k}|,|\hat{h}_{m,k}|^{-1}\big\}\\ &\leq 2^{K^2}\prod_{m,k}\max\big\{|h_{m,k}|,|h_{m,k}|^{-1}\big\}\end{aligned}$$

for $\boldsymbol{H}$ such that $\|\boldsymbol{H}\|_\infty\leq\nu$. Hence,

$$\log(c(\boldsymbol{H},\nu))\mathbb{1}\{\|\boldsymbol{H}\|_\infty\leq\nu\}\leq K^2+\sum_{m,k}\log\big(\max\big\{|h_{m,k}|,|h_{m,k}|^{-1}\big\}\big).$$

Since

$$\mathbb{E}\big(\log\big(\max\big\{|h_{m,k}|,|h_{m,k}|^{-1}\big\}\big)\big)<\infty$$

by assumption on the fading process, this implies that

$$\lim_{\nu\to\infty} \mathbb{E}\big(\log(c(\boldsymbol{H},\nu)); \|\boldsymbol{H}\|_\infty \leq \nu \big) = \mathbb{E}\big(\lim_{\nu\to\infty} \log(c(\boldsymbol{H},\nu)) \big)$$

by dominated convergence. Since $\hat{\boldsymbol{H}}$ converges to $\boldsymbol{H}$ almost surely as $\nu \to \infty$ by the construction of the quantizer, this yields

$$\begin{aligned} \lim_{\nu\to\infty} \mathbb{E}\big(\log(c(\boldsymbol{H},\nu)); \|\boldsymbol{H}\|_\infty \leq \nu \big) &= \sum_{m,k} \mathbb{E}\big(\log\big(\max\big\{ |h_{m,k}|, |h_{m,k}|^{-1} \big\} \big) \big) \\ &= \frac{K^2}{2} \mathbb{E}\big(\log\big(\max\big\{ |h_{1,1}|^2, |h_{1,1}|^{-2} \big\} \big) \big). \end{aligned} \tag{56}$$

It remains to upper bound the expectation over $h_{1,1}$. Since $|h_{1,1}|^2$ has exponential distribution, we have

$$\begin{aligned} \mathbb{E}\big(\log\big(\max\big\{ |h_{1,1}|^2, |h_{1,1}|^{-2} \big\} \big) \big) &= -\int_{s=0}^{1} \exp(-s)\log(s)ds + \int_{s=1}^{\infty} \exp(-s)\log(s)ds \\ &= (\gamma - 2\,\mathrm{Ei}(-1))\log(e) \\ &\leq 1.5, \end{aligned}$$

where γ is the Euler-Mascheroni constant. Combining this with (56) shows that

$$\lim_{\nu\to\infty} \mathbb{E}\big(\log(c(\hat{\boldsymbol{H}})); \|\hat{\boldsymbol{H}}\|_\infty < \infty \big) = \mathbb{E}\big(\lim_{\nu\to\infty} \log(c(\boldsymbol{H},\nu)) \big) \leq \frac{3K^2}{4}.$$

REFERENCES

[1] S. Avestimehr, S. Diggavi, and D. N. C. Tse, "Wireless network information flow: A deterministic approach," *IEEE Transactions on Information Theory*, vol. 57, pp. 1872–1905, Apr. 2011.

[2] S. H. Lim, Y.-H. Kim, A. El Gamal, and S.-Y. Chung, "Noisy network coding," *IEEE Transactions on Information Theory*, vol. 57, pp. 3132–3152, May 2011.

[3] B. Nazer and M. Gastpar, "Compute-and-forward: Harnessing interference through structured codes," *arXiv:0908.2119 [cs.IT]*, Oct. 2011. To appear in IEEE Transactions on Information Theory.

[4] U. Niesen and P. Whiting, "The degrees of freedom of compute-and-forward," *arXiv:1101.2182 [cs.IT]*, Jan. 2011. Submitted to IEEE Transactions on Information Theory.

[5] A. S. Motahari, S. O. Gharan, M.-A. Maddah-Ali, and A. K. Khandani, "Real interference alignment: Exploiting the potential of single antenna systems," *arXiv:0908.2282 [cs.IT]*, Nov. 2009. Submitted to IEEE Transactions on Information Theory.

[6] B. Nazer, M. Gastpar, S. A. Jafar, and S. Vishwanath, "Ergodic interference alignment," in *Proceedings of the International Symposium on Information Theory*, pp. 1769–1773, June 2009.

[7] R. Koetter, M. Effros, and M. Médard, "A theory of network equivalence – Part I: Point-to-point channels," *IEEE Transactions on Information Theory*, vol. 57, pp. 972–995, Feb. 2011.

[8] L. R. Ford and D. R. Fulkerson, "Maximal flow through a network," *Canadian Journal of Mathematics*, vol. 8, pp. 399–404, 1956.

[9] P. Elias, A. Feinstein, and C. E. Shannon, "A note on the maximum flow through a network," *IRE Transactions on Information Theory*, vol. 2, pp. 117–119, Dec. 1956.

[10] R. Ahlswede, N. Cai, S.-Y. R. Li, and R. W. Yeung, "Network information flow," *IEEE Transactions on Information Theory*, vol. 46, pp. 1204–1216, July 2000.

[11] T. M. Cover and A. El Gamal, "Capacity theorems for the relay channel," *IEEE Transactions on Information Theory*, vol. 25, pp. 572–584, Sept. 1979.

[12] G. Kramer, M. Gastpar, and P. Gupta, "Cooperative strategies and capacity theorems for relay networks," *IEEE Transactions on Information Theory*, vol. 51, pp. 3037–3063, Sept. 2005.

[13] A. Sanderovich, O. Somekh, H. V. Poor, and S. Shamai, "Uplink macro diversity of limited backhaul cellular network," *IEEE Transactions on Information Theory*, vol. 55, pp. 3457–3478, Aug. 2009.

[14] B. Schein and R. G. Gallager, "The Gaussian parallel relay network," in *Proceedings of the IEEE International Symposium on Information Theory*, p. 22, June 2000.

[15] J. N. Laneman, D. N. C. Tse, and G. W. Wornell, "Cooperative diversity in wireless networks: Efficient protocols and outage behavior," *IEEE Transactions on Information Theory*, vol. 50, pp. 3062–3080, Dec. 2004.

[16] M. Gastpar and M. Vetterli, "On the capacity of large Gaussian relay networks," *IEEE Transactions on Information Theory*, vol. 51, pp. 765–779, Mar. 2005.

[17] S. Borade, L. Zheng, and R. Gallager, "Amplify-and-forward in wireless relay networks: Rate, diversity, and network size," *IEEE Transactions on Information Theory*, vol. 53, pp. 3302–3318, Oct. 2007.

[18] I. Maric, A. Goldsmith, and M. Médard, "Analog network coding in the high-SNR regime," in *Proceedings of the IEEE Wireless Network Coding Conference*, pp. 1–6, June 2010.

[19] M. P. Wilson, K. Narayanan, H. D. Pfister, and A. Sprintson, “Joint physical layer coding and network coding for bidirectional relaying,” *IEEE Transactions on Information Theory*, vol. 11, pp. 5641–5654, Nov. 2010.

[20] W. Nam, S.-Y. Chung, and Y. H. Lee, “Capacity of the Gaussian two-way relay channel to within $1/2$ bit,” *IEEE Transactions on Information Theory*, vol. 56, pp. 5488–5494, Nov. 2010.

[21] M. R. Aref, *Information Flow in Relay Networks*. PhD thesis, Stanford University, Stanford, CA, Oct. 1981.

[22] N. Ratnakar and G. Kramer, “The multicast capacity of deterministic relay networks with no interference,” *IEEE Transactions on Information Theory*, vol. 52, pp. 2425–2432, June 2006.

[23] R. H. Etkin, D. N. C. Tse, and H. Wang, “Gaussian interference channel capacity to within one bit,” *IEEE Transactions on Information Theory*, vol. 54, pp. 5534–5562, Dec. 2008.

[24] G. Bresler, A. Parekh, and D. N. C. Tse, “The approximate capacity of the many-to-one and one-to-many Gaussian interference channels,” *IEEE Transactions on Information Theory*, vol. 56, pp. 4566–4592, Sept. 2010.

[25] S. Mohajer, S. N. Diggavi, C. Fragouli, and D. N. C. Tse, “Approximate capacity of a class of Gaussian interference-relay networks,” *IEEE Transactions on Information Theory*, vol. 57, pp. 2837–2864, May 2011.

[26] U. Niesen and S. Diggavi, “The approximate capacity of the Gaussian N-relay diamond network,” *arXiv:1008.3813 [cs.IT]*, Aug. 2010. Submitted to IEEE Transactions on Information Theory.

[27] M. A. Maddah-Ali, A. S. Motahari, and A. K. Khandani, “Communication over MIMO X channels: Interference alignment, decomposition, and performance analysis,” *IEEE Transactions on Information Theory*, vol. 54, pp. 3457–3470, Aug. 2008.

[28] V. R. Cadambe and S. A. Jafar, “Interference alignment and the degrees of freedom for the K-user interference channel,” *IEEE Transactions on Information Theory*, vol. 54, pp. 3425–3441, Aug. 2008.

[29] S. Sridharan, A. Jafarian, S. Vishwanath, S. A. Jafar, and S. Shamai, “A layered lattice coding scheme for a class of three user Gaussian interference channels,” in *46th Annual Allerton Conference on Communications, Control, and Computing*, pp. 531–538, Sept. 2008.

[30] S.-W. Jeon, S.-Y. Chung, and S. A. Jafar, “Approximate capacity of a class of multi-source Gaussian relay networks,” in *Proceedings of the IEEE Information Theory Workshop*, pp. 1–5, Aug. 2010.

[31] T. Gou, S. A. Jafar, S.-W. Jeon, and S.-Y. Chung, “Aligned interference neutralization and the degrees of freedom of the 2x2x2 interference channel,” *arXiv:1012.2350*, Dec. 2010. Submitted to IEEE Transactions on Information Theory.

[32] I. Shomorony and A. S. Avestimehr, “Two-unicast wireless networks: Characterizing the degrees-of-freedom,” *arXiv:1102.2498 [cs.IT]*, Mar. 2011. Submitted to IEEE Transactions on Information Theory.

[33] C. Wang, T. Gou, and S. A. Jafar, “Multiple unicast capacity of 2-source 2-sink networks,” *arXiv:1104.0954 [cs.IT]*, Apr. 2011. Submitted to IEEE GLOBECOM 2011.

[34] R. Zamir, S. Shamai, and U. Erez, “Nested linear/lattice codes for structured multiterminal binning,” *IEEE Transactions on Information Theory*, vol. 48, pp. 1250–1276, June 2002.

[35] R. Zamir, “Lattices are everywhere,” in *Proceedings of the 4th Annual Workshop on Information Theory and its Applications*, pp. 392–421, Feb. 2009.

[36] T. Philosof, R. Zamir, U. Erez, and A. Khisti, “Lattice strategies for the dirty multiple access channel,” *arXiv:0904.1892 [cs.IT]*, Apr. 2009. Submitted to IEEE Transactions on Information Theory.

[37] W. Nam, S.-Y. Chung, and Y. H. Lee, “Nested lattice codes for Gaussian relay networks with interference,” *arXiv:0902.2436 [cs.IT]*, Feb. 2009. Submitted to IEEE Transactions on Information Theory.

[38] A. Özgür and S. Diggavi, “Approximately achieving Gaussian relay network capacity with lattice codes,” in *Proceedings of the IEEE International Symposium on Information Theory*, pp. 669–673, June 2010.

[39] R. Durret, *Probability: Theory and Examples*. Duxbury Press, third ed., 2004.

[40] U. Niesen, “Interference alignment in dense wireless networks,” *IEEE Transactions on Information Theory*, vol. 57, pp. 2889–2901, May 2011.

[41] T. Cover and J. Thomas, *Elements of Information Theory*. Wiley-Interscience, 1991.

[42] A. J. Goldsmith and P. P. Varaiya, “Capacity of fading channels with channel side information,” *IEEE Transactions on Information Theory*, vol. 43, pp. 1986–1992, Nov. 1997.

[43] U. Erez and R. Zamir, “Achieving $\frac{1}{2}\log(1+\mathrm{SNR})$ on the AWGN channel with lattice encoding and decoding,” *IEEE Transactions on Information Theory*, vol. 50, pp. 2293–2314, Oct. 2004.